Supplementary Information

for

Solvent Dependent Hindered Rotation versus Epimerization in Axially Chiral Thiohydantoin Derivatives: An Experimental and a Computational Study

Sule Erol Gunal[a], Ipek Azizoglu[a], Oya Arica[a], Zeynep Pinar Haslak[a], Viktorya Aviyente[a]*, Ilknur Dogan[a]*

[a] *Department of Chemistry, Bogaziçi University, Bebek, Istanbul, Turkey*

Table of Contents

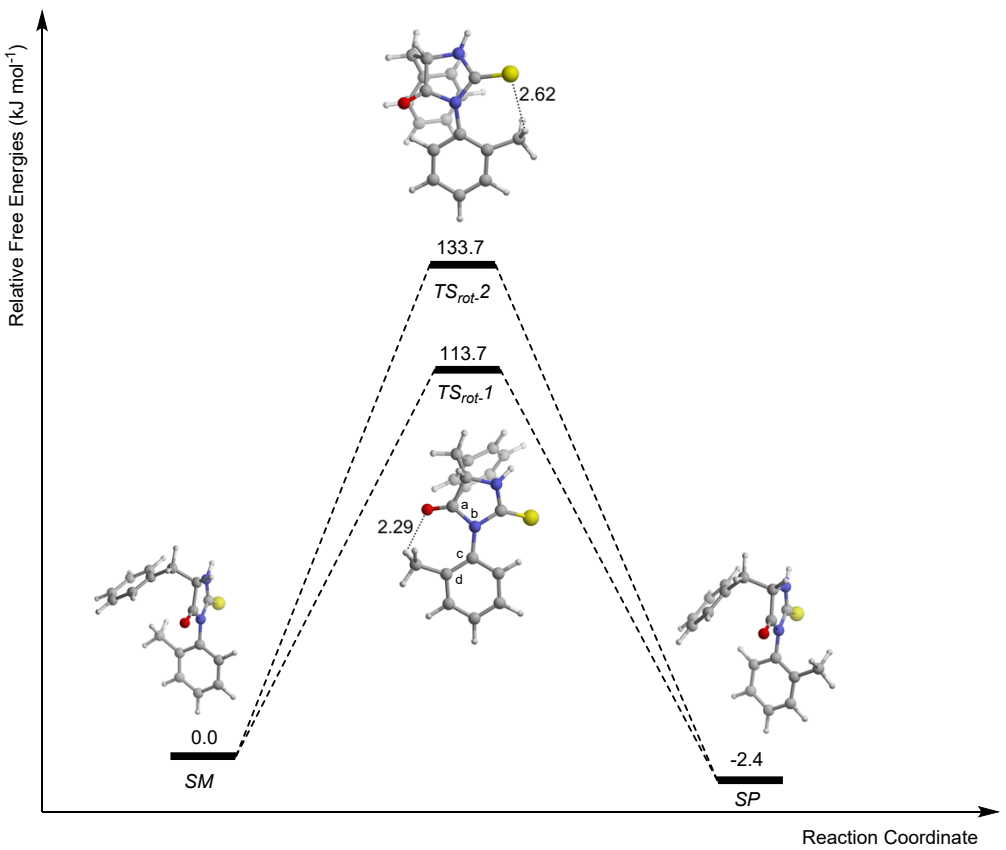

Fig. S1 Potential energy surfaces for the **SM** to **SP** transformations of compound **1** around C_{aryl}-N_{sp2} bond through exo-cyclic oxygen site (***TS$_{rot}$-1***) and exo-cyclic sulfur site (***TS$_{rot}$-2***).

Geometrical features and energetics of the compounds in Figure S1:

For ***SM*** enantiomer of 5-benzyl-3-(*o*-tolyl)-2-thiohydantoin (compound **1**) the minima was located on the potential energy surface at a dihedral angle of $\theta_{a\text{-}b\text{-}c\text{-}d}$ = 96.27°. The rotational transition state structure ***TS$_{rot}$-1***, where the *o*-aryl substituent methyl rotates via the exo-cyclic oxygen has $\theta_{a\text{-}b\text{-}c\text{-}d}$ = -0.24° and the two rings are flat and coplanar because of the electron delocalization. C_{aryl}-N_{sp2} bond elongates from 1.433 Å to 1.458 Å in going from ground state structure ***SM*** to transition state structure ***TS$_{rot}$-1***. $\theta_{a\text{-}b\text{-}c\text{-}d}$ was calculated to be -174.24° in ***TS$_{rot}$-2*** structure, where the *o*-aryl substituent methyl rotates via the exo-cyclic sulfur atom and the two rings slightly deviate from planarity since larger S atom induces steric repulsion with the *o*-aryl methyl group. C_{aryl}-N_{sp2} bond elongates from 1.433 Å to 1.468 Å in going from ground state structure ***SM*** to transition state structure ***TS$_{rot}$-2***. As a consequence, ***TS$_{rot}$-2*** has a higher rotational energy barrier than ***TS$_{rot}$-1***. In the ground state of ***SP***, the thermodynamically favored product, $\theta_{a\text{-}b\text{-}c\text{-}d}$ = -78.61°. Compared to ***SM***, in ***SP***, *o*-aryl methyl and benzyl group at *R* position do not face each other which is sterically a more favorable orientation.

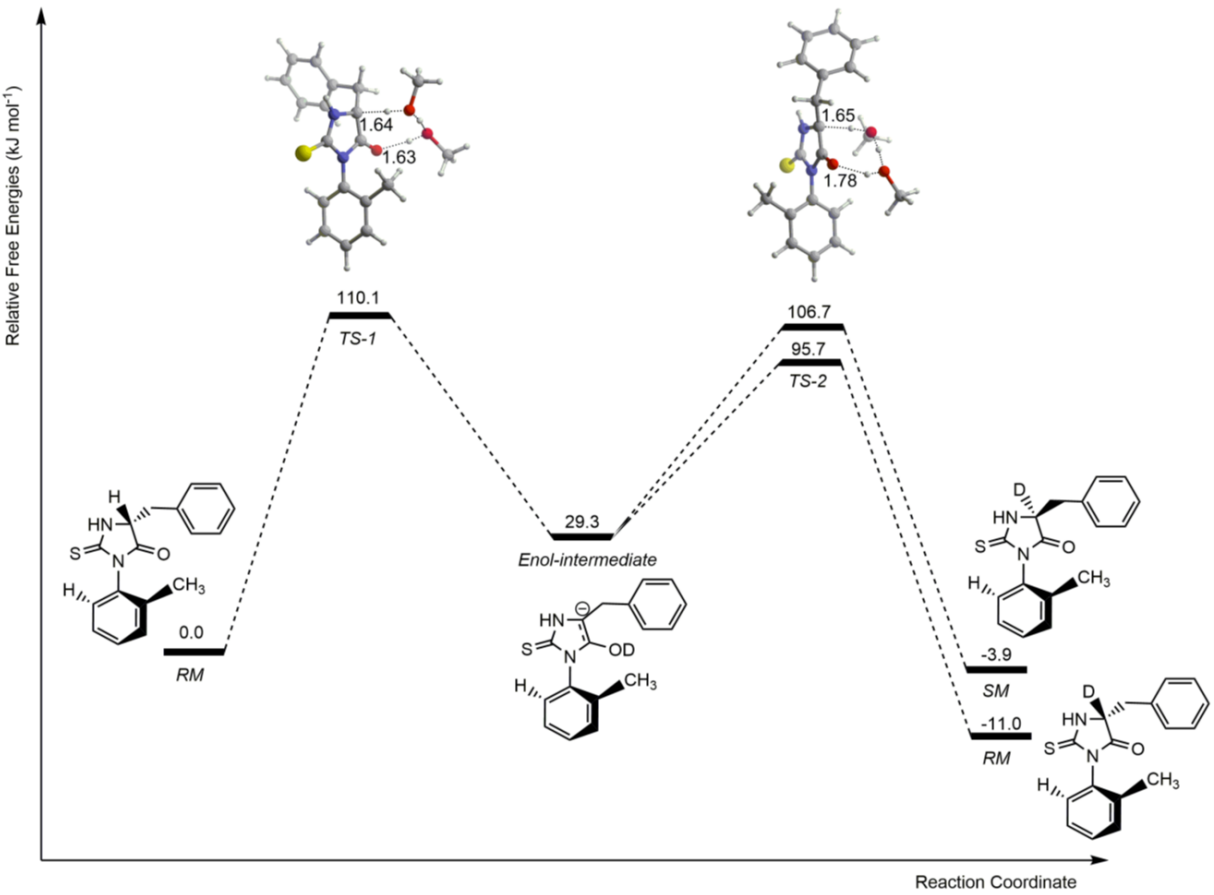

Fig. S2 Free energy profile for the epimerization process of 5-benzyl-3-(*o*-tolyl)-2-thiohydantoin (compound 1) in the presence of CD_3OD molecules.

Geometrical features and energetics of the compounds in Figure S2:

For the starting ground state conformation of ***RM*** enantiomer of 5-benzyl-3-(*o*-tolyl)-2-thiohydantoin (compound **1**) in the presence of two CD_3OD molecules, the minima was located on the potential energy surface at a dihedral angle of $\theta_{a\text{-}b\text{-}c\text{-}d}$ = 74.36°. The transition state structure (**TS-1**) for deprotonation of ***RM*** embodies an eight-membered cyclic structure involving triple proton transfer. CD_3OD_1 abstracts the proton at the stereocenter C5 with a bond length of 1.64 Å and transfers its deuterium which is attached to oxygen atom to CD_3OD_2 while another deuterium transfer occurs from CD_3OD_2 to carbonyl oxygen on 5-membered ring of compound **1** with a bond length of 1.63 Å, yielding the enolate intermediate. In ***TS-1*** structure $\theta_{a\text{-}b\text{-}c\text{-}d}$ = 76.66°. C_{aryl}-N_{sp2} bond shortens from 1.432 Å to 1.429 Å, C=O bond elongates from 1.210 Å to 1.253 Å and C5-$C_{benzene}$ bond shortens from 1.546 Å to 1.516 Å in going from ground state structure ***RM*** to transition state structure ***TS-1***. In the ***Enol-intermediate***, $\theta_{a\text{-}b\text{-}c\text{-}d}$ = 79.43°, d(C_{aryl}-N_{sp2}) = 1.431 Å, d(C=O) = 1.335 Å and d(C5-$C_{benzene}$) = 1.492 Å. In the deuteration step of C5 to yield the deuterated ***SM*** stereoisomer (***TS-2***, $\theta_{a\text{-}b\text{-}c\text{-}d}$ = 84.32°, upper path in Fig. S2), C5 abstracts the deuterium from CD_3OD_1, which approaches from *re*-face of the compound,

with a bond length of 1.65 Å while CD_3OD_1 picks a deuterium from CD_3OD_2 and CD_3OD_2 abstracts the deuterium from carbonyl oxygen on 5-membered ring of compound **1** with a bond length of 1.78 Å. In going from ground state structure ***Enol-intermediate*** to transition state structure ***TS-2*** to yield ***SM*** stereoisomer, C_{aryl}-N_{sp2} bond shortens from 1.431 Å to 1.429 Å, C=O bond shortens from 1.335 Å to 1.248 Å and C5-$C_{benzene}$ bond elongates from 1.492 Å to 1.505 Å. For the ground state conformation of deuterated ***SM*** enantiomer in the presence of two CD_3OD molecules, the minima was located on the potential energy surface at a dihedral angle of $\theta_{a\text{-}b\text{-}c\text{-}d}$ = 85.33°.On the other hand, to yield the deuteurated ***RM*** stereoisomer, deuteriation (***TS-2***, $\theta_{a\text{-}b\text{-}c\text{-}d}$ = 76.09°, lower path in Fig. S2) occurs from the *si*-face of the compound, with shorter C5$\cdots_1$D—OCD_3 (1.64 Å) and O$\cdots_2$D—OCD_3 (1.62 Å) bonds. In going from ground state structure of ***Enol-intermediate*** to transition state structure ***TS-2*** to yield ***RM*** stereoisomer, C_{aryl}-N_{sp2} bond shortens from 1.431 Å to 1.429 Å, C=O bond shortens from 1.335 Å to 1.253 Å and C5-$C_{benzene}$ bond elongates from 1.492 Å to 1.511 Å. For the ground state conformation of deuterated ***RM*** enantiomer in the presence of two CD_3OD molecules, the minima was located on the potential energy surface at a dihedral angle of $\theta_{a\text{-}b\text{-}c\text{-}d}$ = 75.32°.

Table S1. Experimental and calculated (*) epimerization barriers for the forward $\Delta G^{\neq}_{f}$, and the reverse $\Delta G^{\neq}_{r}$ ($\Delta G^{\neq}$, *kJ/mol*) reactions (M06-2X/6-311+G**) and the corresponding experimentally determined rate constants (k, s^{-1}) for compounds **1-4**, in ethanol.

Compound	**T (°C)**	**Stereoisomer conversion**	$\Delta G^{\neq}_{f}$	$\Delta G^{\neq}_{r}$	k_f	k_r
1	25	**SM** to **RM**	100.4±1.2 106.1*	99.3±1.2	1.59×10^{-5}	2.41×10^{-5}
	25	**RM** to **SM**	100.5±1.2 107.4*	100.5±1.2	1.51×10^{-5}	1.49×10^{-5}
2	40	**RP** to **SP**	100.0±3.2	101.9±3.2	1.36×10^{-4}	6.43×10^{-5}
	40	**SP** to **RP**	104.6±3.2	102.7±3.2	2.26×10^{-5}	4.74×10^{-5}
	40	**RM** to **SM**	105.7±3.2	104.3±3.2 105.4*	1.48×10^{-5}	2.52×10^{-5}
3	25	**RP** to **SP**	99.4±1.8	100.2±1.8	2.30×10^{-5}	1.70×10^{-5}
	25	**SP** to **RP**	102.0±1.8	101.1±1.8	8.25×10^{-6}	1.18×10^{-6}
	25	**RM** to **SM**	102.0±1.8	101.1±1.8	8.28×10^{-6}	1.17×10^{-6}
	25	**SM** to **RM**	100.5±1.8 99.3*	100.6±1.8	1.53×10^{-5}	1.47×10^{-5}
4	40	**RP** to **SP**	102.1±0.1	103.1±0.1	5.97×10^{-5}	4.04×10^{-5}
	40	**SP** to **RP**	103.2±0.1	102.1±0.1	3.98×10^{-5}	6.02×10^{-5}
	40	**RM** to **SM**	103.0±0.1	102.2±0.1 101.6*	4.27×10^{-5}	5.73×10^{-5}

Table S2. 3D representations of the GS and TS structures of compounds **1-4** and corresponding α, β and θ values (calculated at M062X/6-311+G** level of theory).

COMPOUND 1 **R_1:** -benzyl **X:** -CH_3	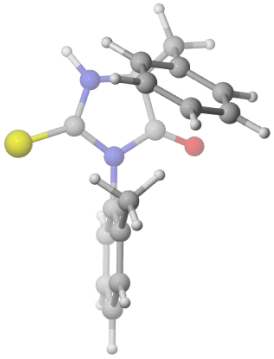 ***SM***	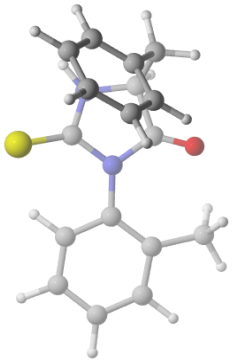 ***TS-S***	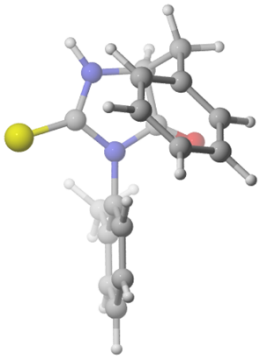 ***SP***
$\theta_{c\text{-}d\text{-}e\text{-}f}$ **α** **β**	96.3° 126.5° 120.7°	-0.2° 128.5° 129.9°	-78.6° 126.5° 120.7°
COMPOUND 1 **R_1:** -benzyl **X:** -CH_3	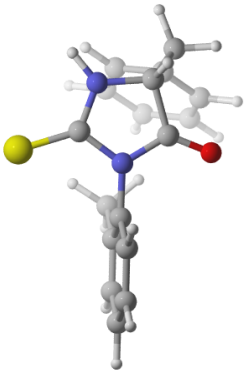 ***RP***	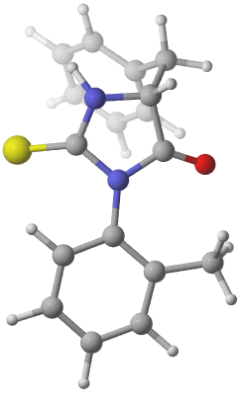 ***TS_{rot}-1***	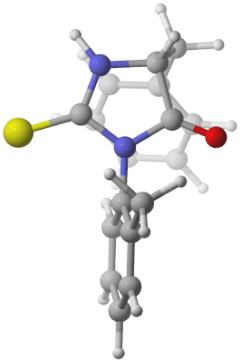 ***RM***
$\theta_{c\text{-}d\text{-}e\text{-}f}$ **α** **β**	-96.3° 126.5° 120.7°	0.2° 128.5° 129.9°	78.6° 126.5° 120.7°
COMPOUND 2 **R_1:** -benzyl **X:** -Br	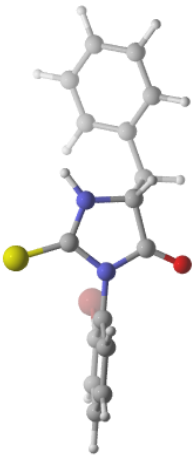	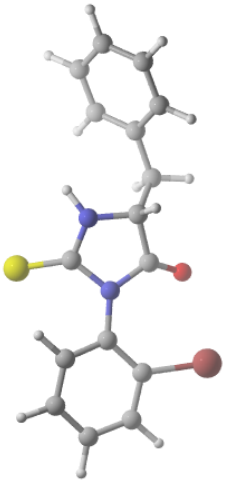	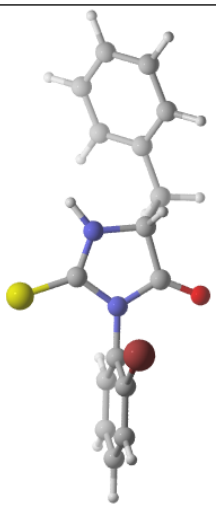

	RP	***TS_{rot}-1***	***RM***
$\theta_{c\text{-}d\text{-}e\text{-}f}$ **α** **β**	-82.1º 126.3º 119.8º	-4.5º 128.0º 128.8º	80.1º 126.3º 119.9º
COMPOUND 3 **R_1:** -isobutyl **X:** -CH_3	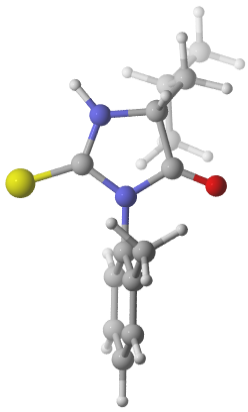	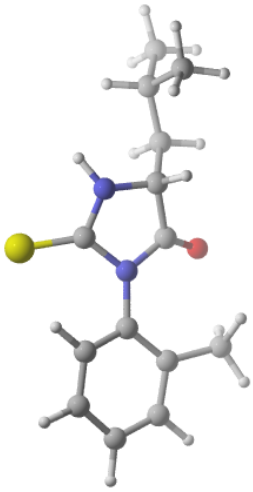	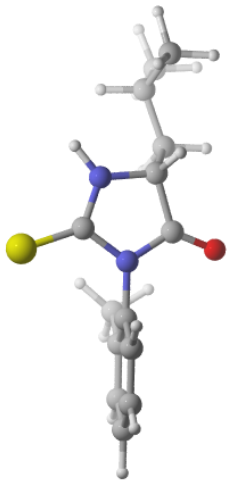
	RM	***TS_{rot}-1***	***RP***
$\theta_{c\text{-}d\text{-}e\text{-}f}$ **α** **β**	75.7º 126.2º 120.9º	-0.7º 128.1º 129.5º	-78.8º 126.2º 120.6º
COMPOUND 4 **R_1:** -isobutyl **X:** -Br	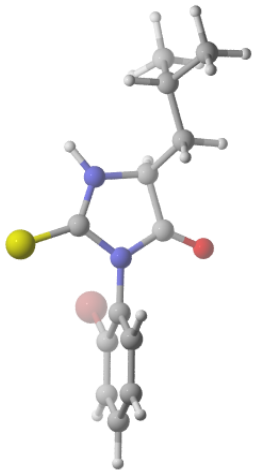	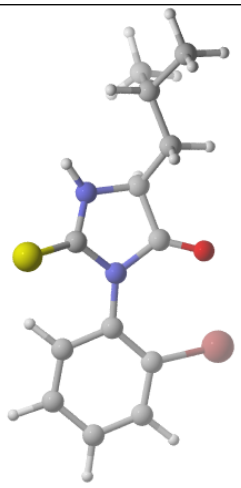	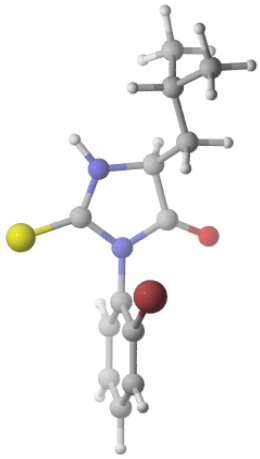
	SP	***TS_{rot}-1***	***SM***
$\theta_{c\text{-}d\text{-}e\text{-}f}$ **α** **β**	-82.1º 126.1º 119.9º	3.4º 127.8º 128.7º	82.9º 126.1º 119.8º

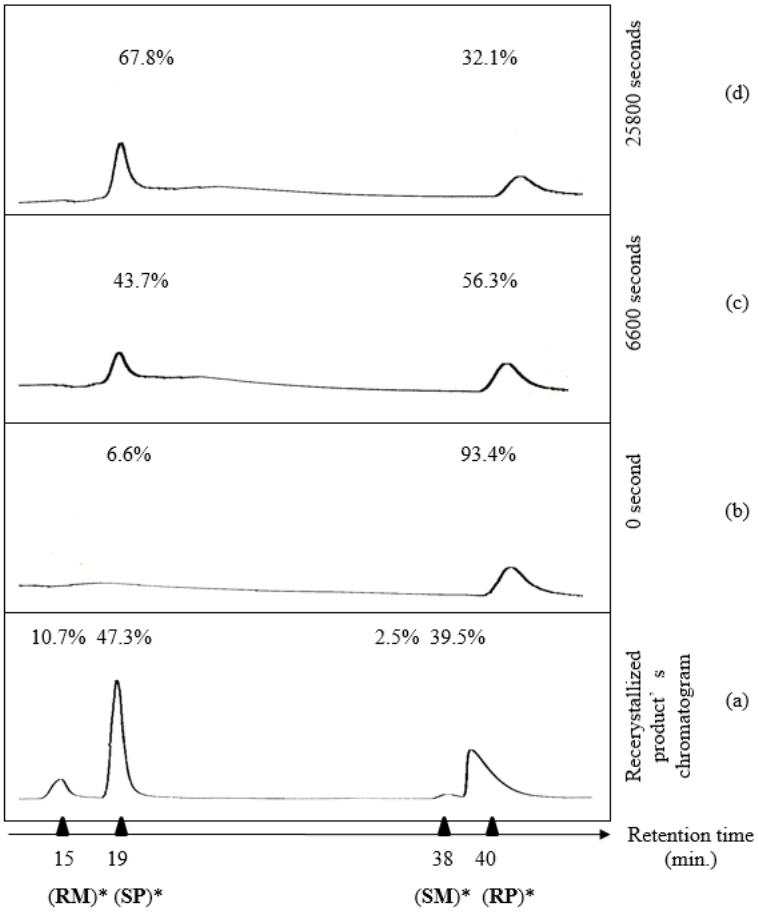

Fig. S3 HPLC chromatograms of 5-benzyl-3-(*o*-bromophenyl)-2-thiohydantoin **(2)** (ChiralPak IC as the stationary phase, 95:5 Hex:EtOH as the eluent, flow rate : 0.8 ml/min, column temperature: 7°C) (a) the recrystallized product which shows the presence of four isomers, (b) the micropreparatively resolved **RP**, (c-d) conversion of **RP** to **SP** with time in **ethanol** at 313 K. (*) The assignments have been done with comparison by the ^{1}H-NMR spectrum.

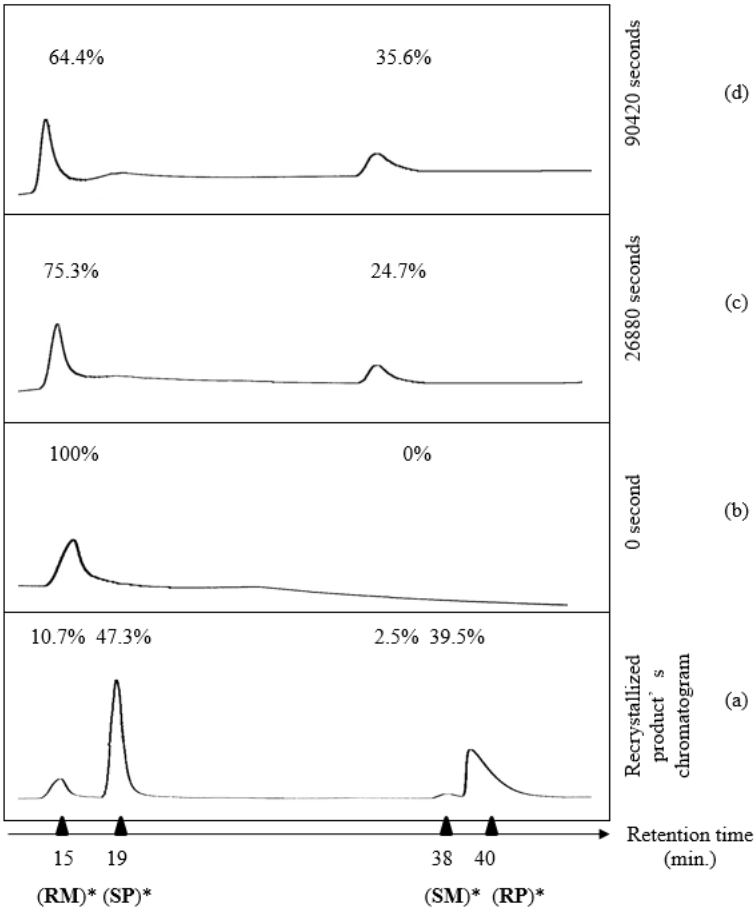

Fig. S4 HPLC chromatograms of 5-benzyl-3-(*o*-bromophenyl)-2-thiohydantoin **(2)** (ChiralPak IC as the stationary phase, 95:5 Hex:EtOH as the eluent, flow rate : 0.8 ml/min, column temperature: 7°C) (a) the recrystallized product which shows the presence of four isomers, (b) the micropreparatively resolved **RM**, (c-d) conversion of **RM** to **SM** with time in **ethanol** at 313 K. (*) The assignments have been done with comparison by the ^{1}H-NMR spectrum.

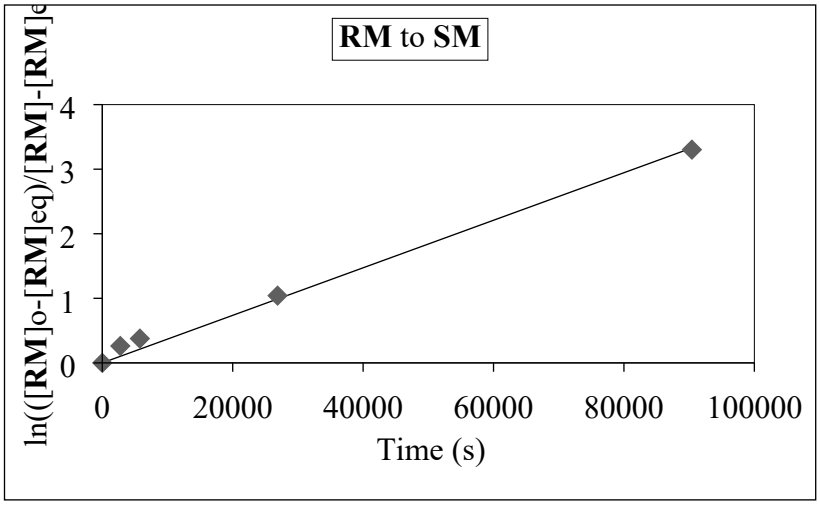

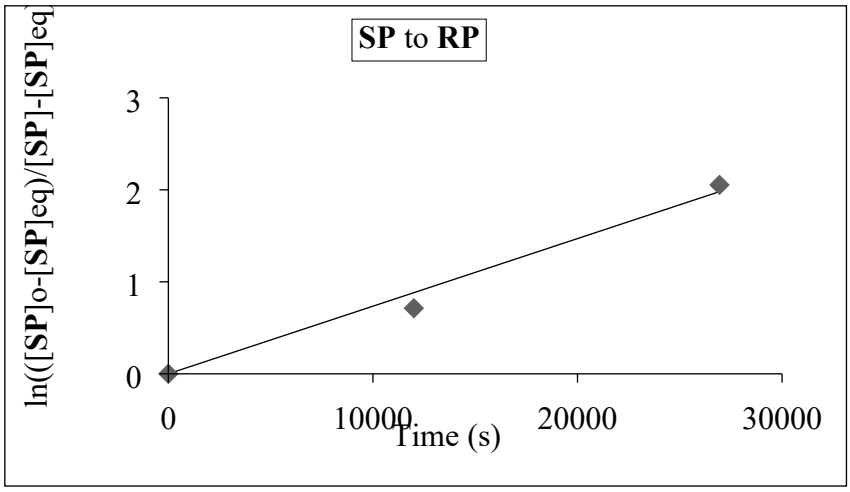

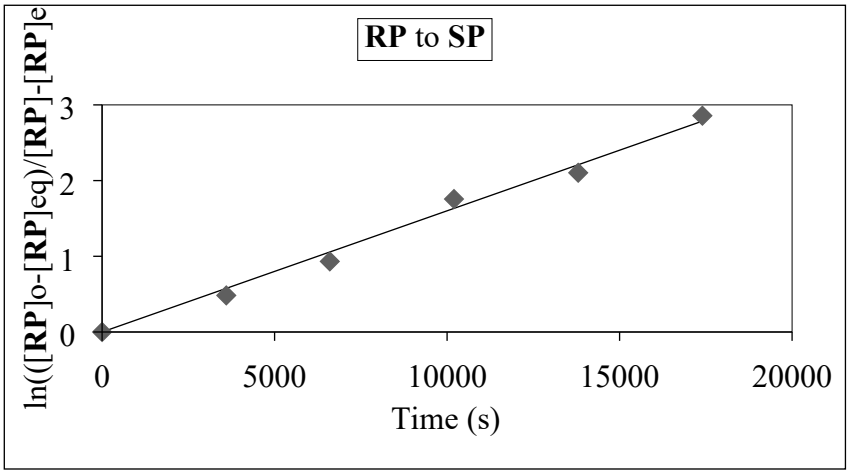

Fig. S5 The plot of ln(([**RM**]o-[**RM**]eq)/[**RM**]-[**RM**]eq)) , ln(([**SP**]o-[**SP**]eq)/[**SP**]-[**SP**]eq)) , ln(([**RP**]o-[**RP**]eq)/[**RP**]-[**RP**]eq)) , versus time at 313 K in **ethanol** for 5-benzyl-3-(*o*-bromophenyl)-2-thiohydantoin **(2)**.

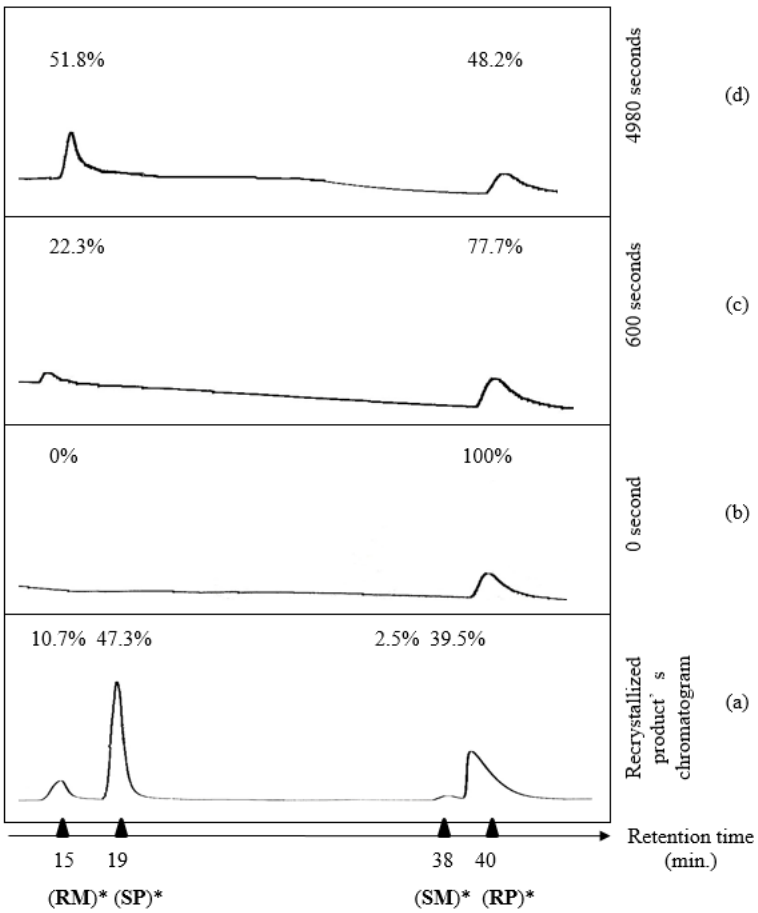

Fig. S6 HPLC chromatograms of 5-benzyl-3-(*o*-bromophenyl)-2-thiohydantoin **(2)** (ChiralPak IC as the stationary phase, 95:5 Hex:EtOH as the eluent, flow rate : 0.8 ml/min, column temperature: 7°C) (a) the recrystallized product which shows the presence of four isomers, (b) the micropreparatively resolved **RP**, (c-d) conversion of **RP** to **RM** with time in **toluene** at 383 K. (*) The assignments have been done with comparison by the ^{1}H-NMR spectrum.

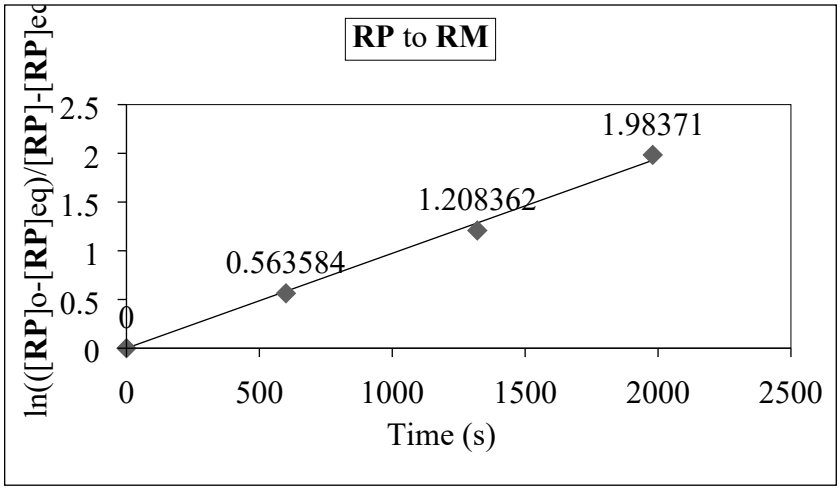

Fig. S7 The plot of ln(([**RP**]o-[**RP**]eq)/[**RP**]-[**RP**]eq)) versus time at 383 K in toluene for 5-benzyl-3-(*o*-bromophenyl)-2-thiohydantoin **(2)** .

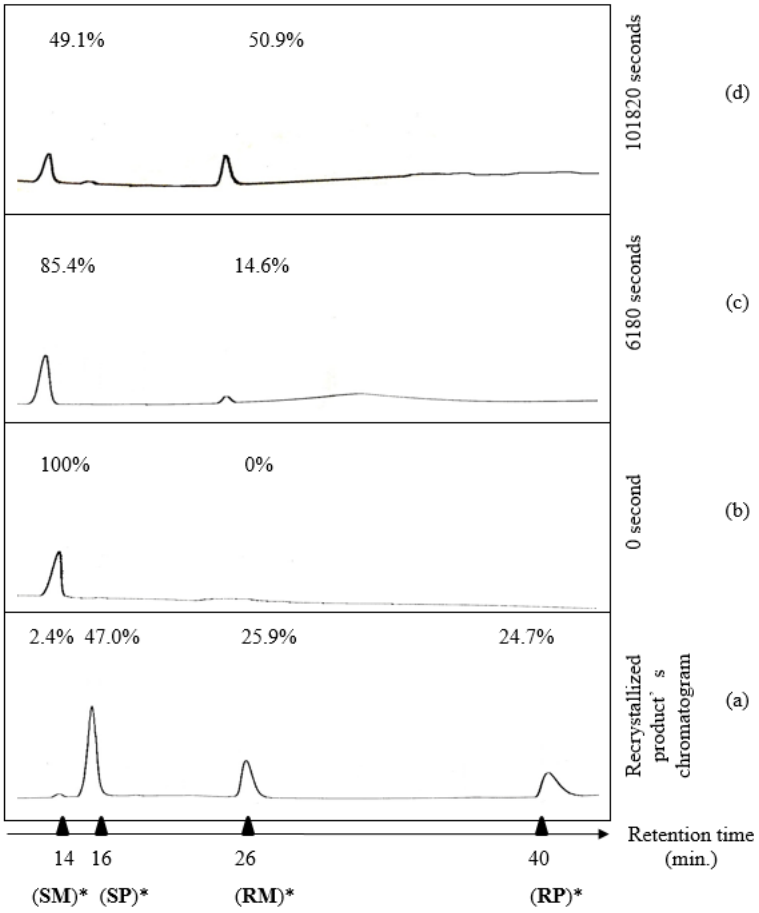

Fig. S8 HPLC chromatograms of 5-isobutyl-3-(*o*-tolyl)-2-thiohydantoin **(3)** (ChiralPak IB as the stationary phase, 95:5 Hex:EtOH as the eluent, flow rate : 0.8 ml/min, column temperature: 7°C) (a) the recrystallized product which shows the presence of four isomers, (b) the micropreparatively resolved **SM**, (c-d) conversion of **SM** to **RM** with time in **ethanol** at 298 K. (*) The assignments have been done with comparison by the ^{1}H-NMR spectrum.

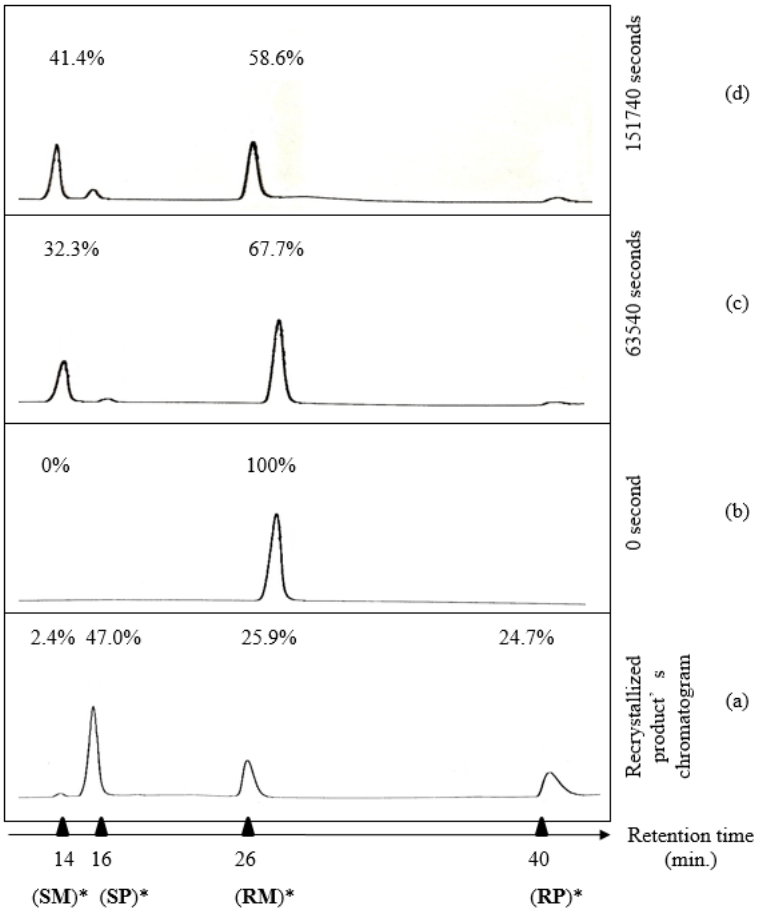

Fig. S9 HPLC chromatograms of 5-isobutyl-3-(*o*-tolyl)-2-thiohydantoin **(3)** (ChiralPak IB as the stationary phase, 95:5 Hex:EtOH as the eluent, flow rate: 0.8 ml/min, column temperature : 7°C) (a) the recrystallized product which shows the presence of four isomers, (b) the micropreparatively resolved **RM**, (c-d) conversion of **RM** to **SM** with time in **ethanol** at 298 K. (*) The assignments have been done with comparison by the ^{1}H-NMR spectrum.

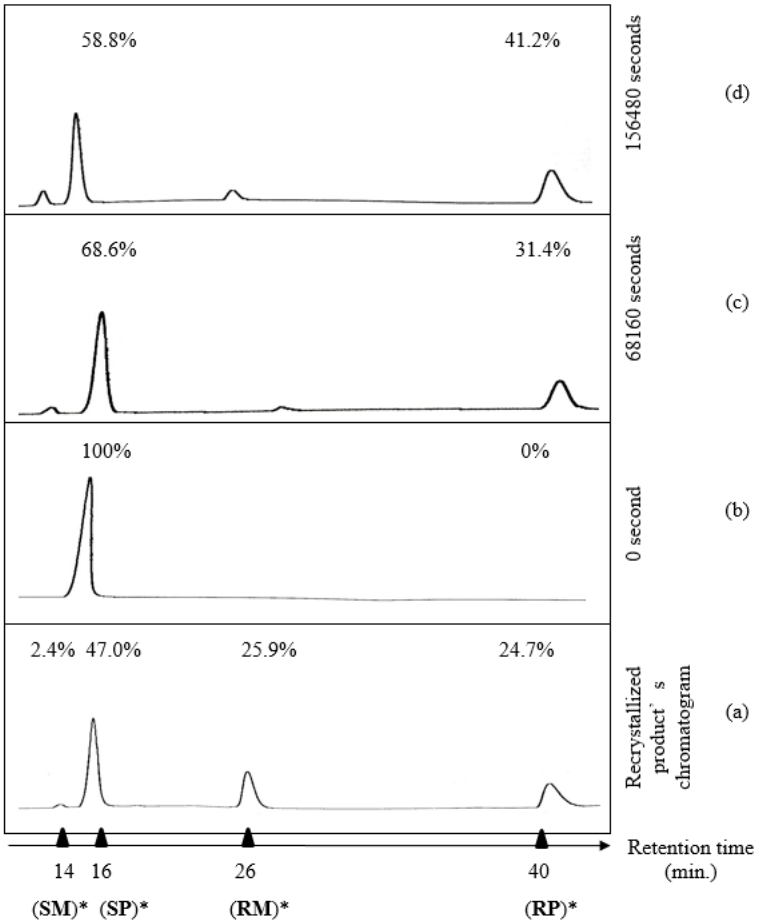

Fig. S10 HPLC chromatograms of 5-isobutyl-3-(*o*-tolyl)-2-thiohydantoin **(3)** (ChiralPak IB as the stationary phase, 95:5 Hex:EtOH as the eluent, flow rate : 0.8 ml/min, column temperature: 7°C) (a) the recrystallized product which shows the presence of four isomers, (b) the micropreparatively resolved **SP**, (c-d) conversion of **SP** to **RP** with time in **ethanol** at 298 K. (*) The assignments have been done with comparison by the ^{1}H-NMR spectrum.

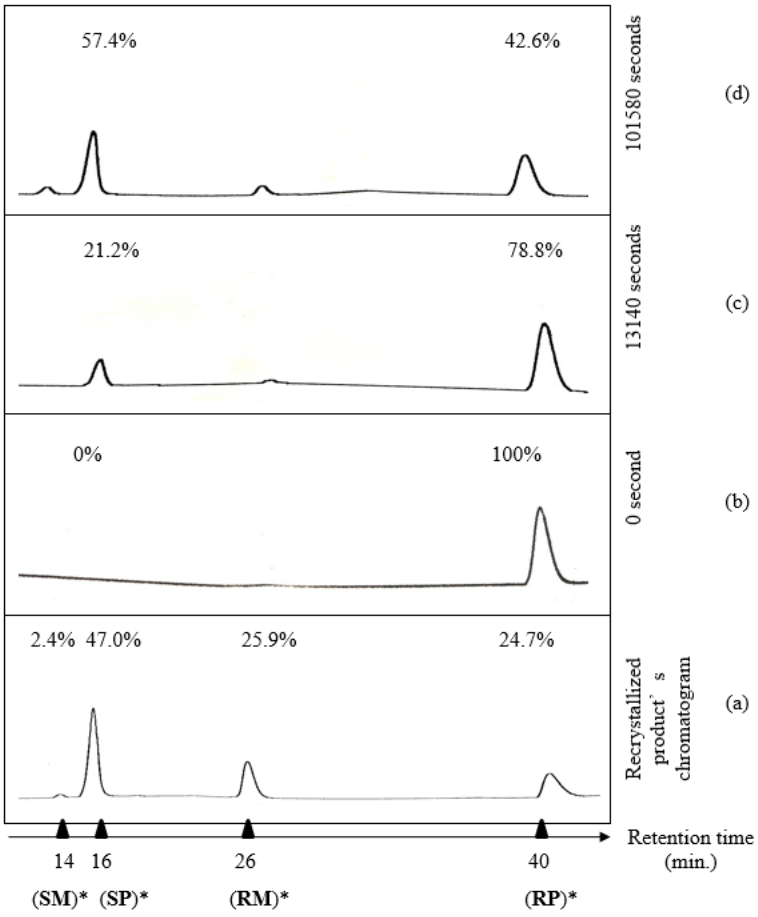

Fig. S11 HPLC chromatograms of 5-isobutyl-3-(*o*-tolyl)-2-thiohydantoin **(3)** (ChiralPak IB as the stationary phase, 95:5 Hex:EtOH as the eluent, flow rate : 0.8 ml/min, column temperature: 7°C) (a) the recrystallized product which shows the presence of four isomers, (b) the micropreparatively resolved **RP**, (c-d) conversion of **RP** to **SP** with time in **ethanol** at 298 K. (*) The assignments have been done with comparison by the ^{1}H-NMR spectrum.

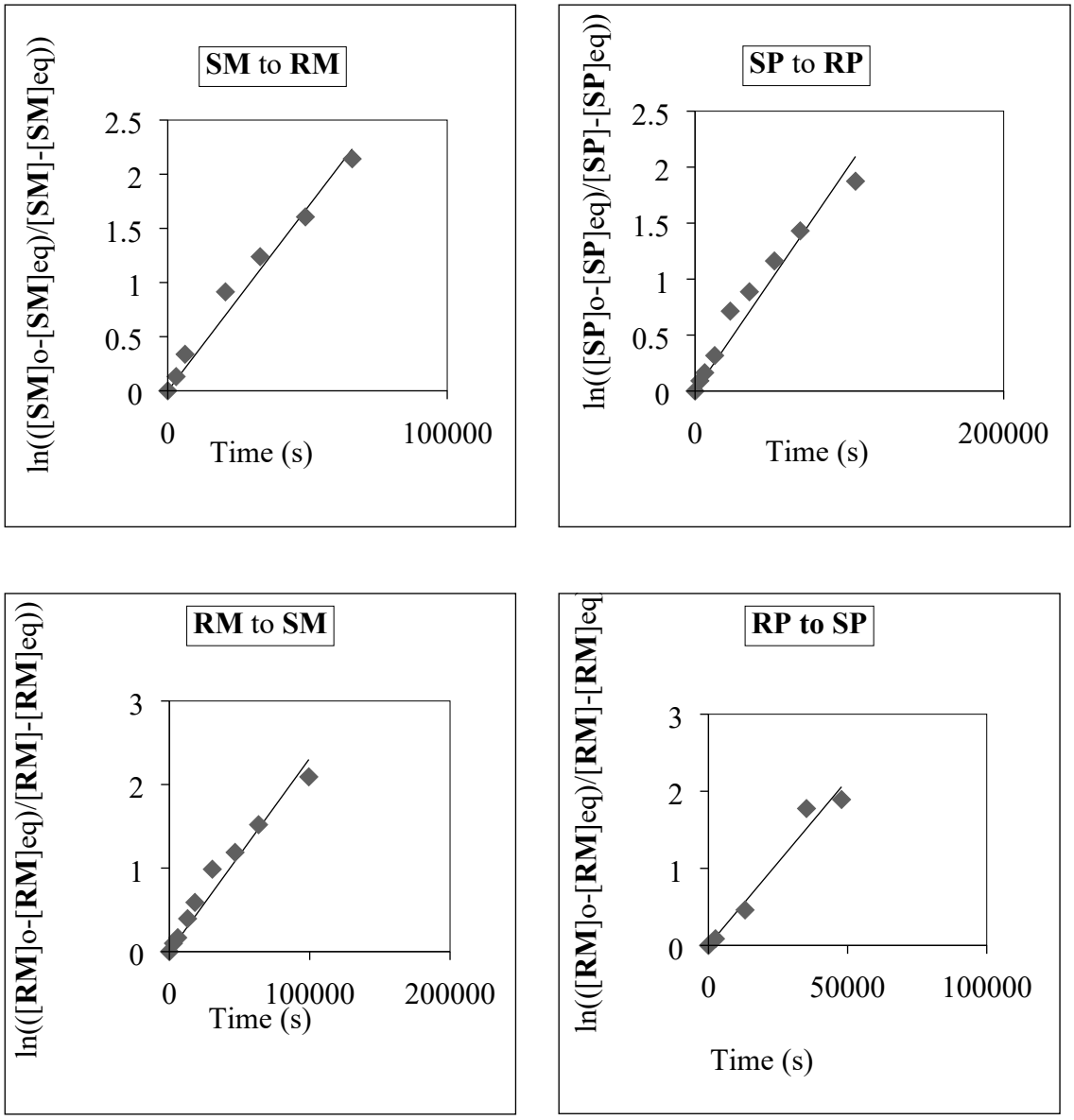

Fig. S12 The plot of ln(([**SM**]o-[**SM**]eq)/[**SM**]-[**SM**]eq)) , ln(([**SP**]o-[**SP**]eq)/[**SP**]-[**SP**]eq)) , ln(([**RM**]o-[**RM**]eq)/[**RM**]-[**RM**]eq)) , ln(([**RP**]o-[**RP**]eq)/[**RP**]-[**RP**]eq)) , versus time in **ethanol** at 298 K for 5-isobutyl-3-(*o*-tolyl)-2-thiohydantoin **(3)**.

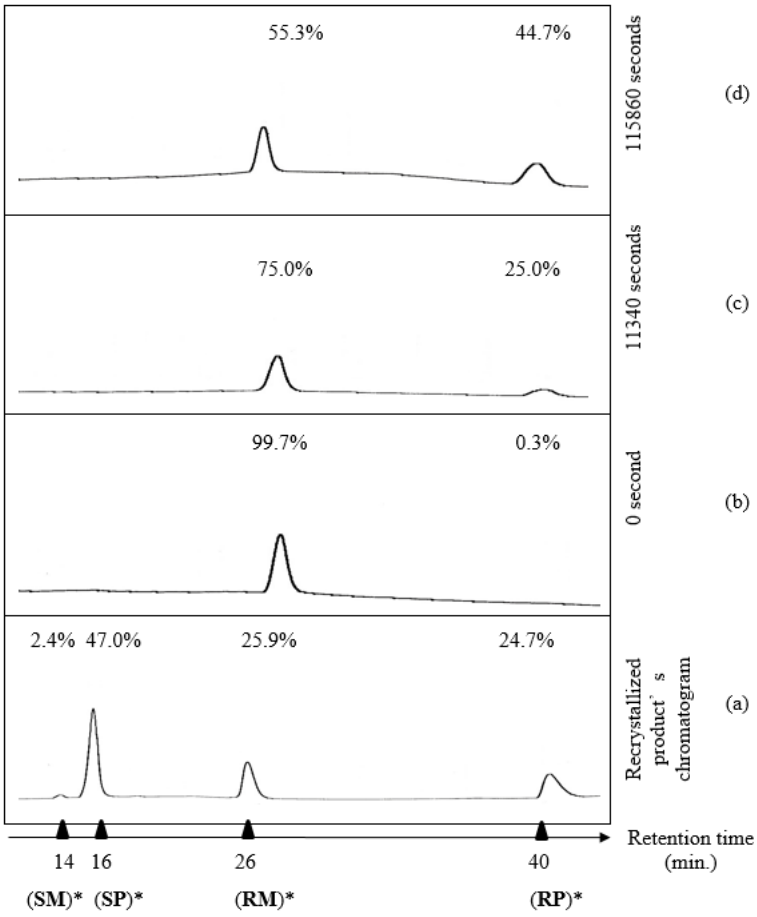

Fig. S13 HPLC chromatograms of 5-isobutyl-3-(*o*-tolyl)-2-thiohydantoin **(3)** (ChiralPak IB as the stationary phase, 95:5 Hex:EtOH as the eluent, flow rate : 0.8 ml/min, column temperature: 7°C) (a) the recrystallized product which shows the presence of four isomers, (b) the micropreparatively resolved **RM**, (c-d) conversion of **RM** to **RP** with time in **toluene** at 313 K. (*) The assignments have been done with comparison by the ^{1}H-NMR spectrum.

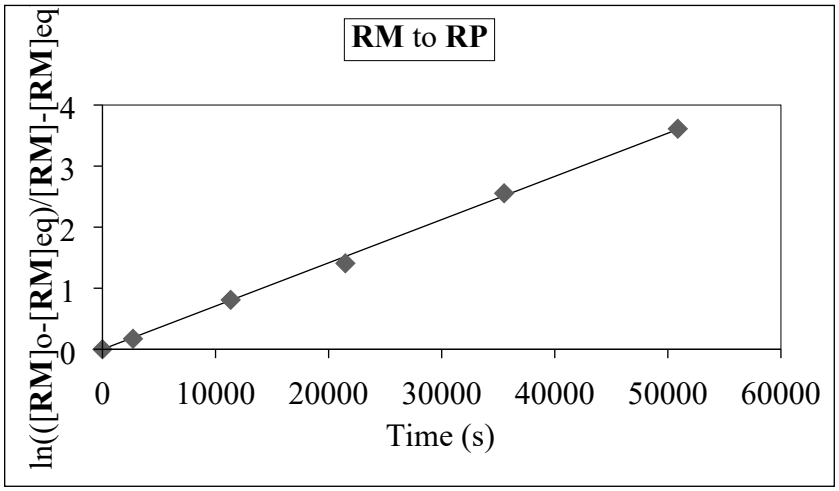

Fig. S14 The plot of ln(([**RM**]o-[**RM**]eq)/[**RM**]-[**RM**]eq)) versus time in **toluene** at 313 K for 5-isobutyl-3-(o-tolyl)-2-thiohydantoin**(3)**.

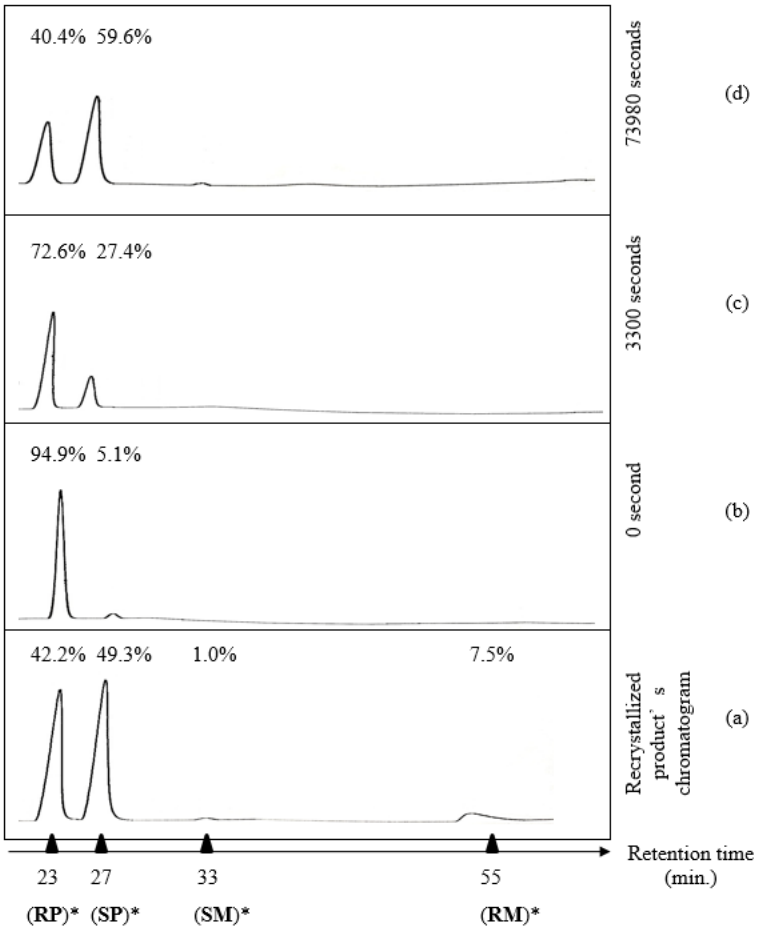

Fig. S15 HPLC chromatograms of 5-isobutyl-3-(*o*-bromophenyl)-2-thiohydantoin **(4)** (ChiralPak IA as the stationary phase, 95:5 Hex:EtOH as the eluent, flow rate : 0.8 ml/min, column temperature: 7°C) (a) the recrystallized product which shows the presence of four isomers, (b) the micropreparatively resolved **RP**, (c-d) conversion of **RP** to **SP** with time in **ethanol** at 313 K. (*) The assignments have been done with comparison by the ^{1}H-NMR spectrum.

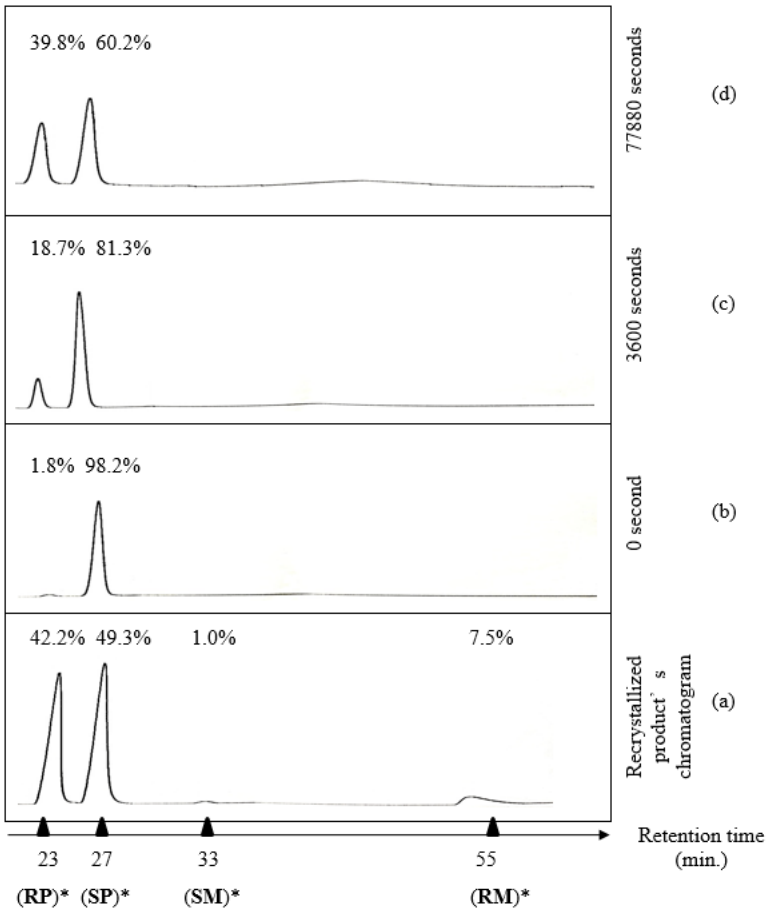

Fig. S16 HPLC chromatograms of 5-isobutyl-3-(*o*-bromophenyl)-2-thiohydantoin **(4)** (ChiralPak IA as the stationary phase, 95:5 Hex:EtOH as the eluent, flow rate : 0.8 ml/min, column temperature: 7°C) (a) the recrystallized product which shows the presence of four isomers, (b) the micropreparatively resolved **SP**, (c-d) conversion of **SP** to **RP** with time in **ethanol** at 313 K. (*) The assignments have been done with comparison by the ^{1}H-NMR spectrum.

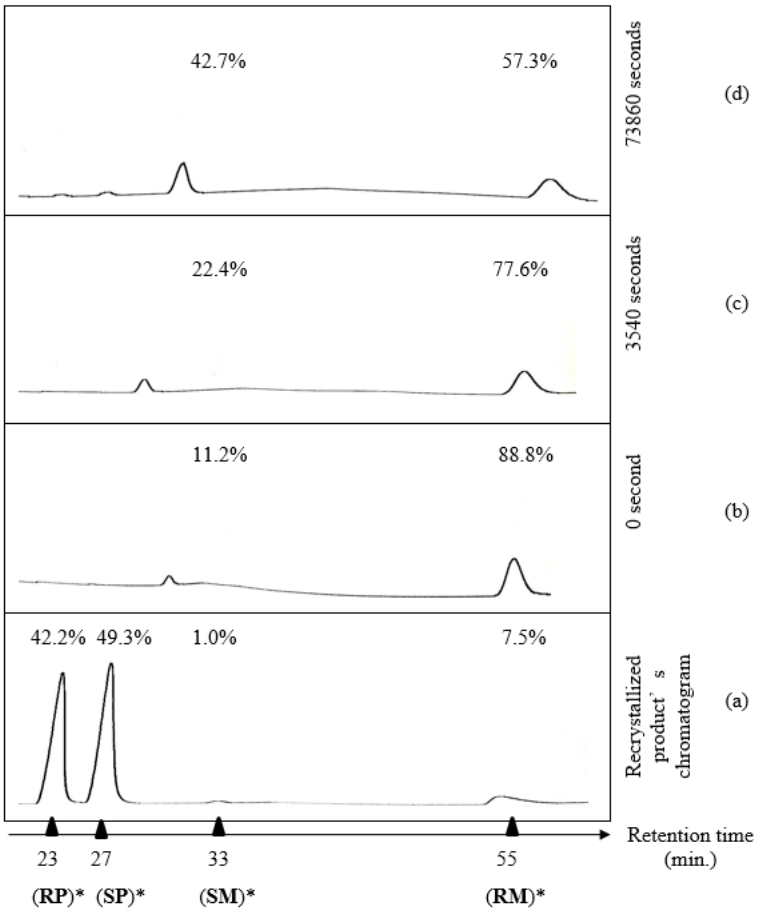

Fig. S17 HPLC chromatograms of 5-isobutyl-3-(*o*-bromophenyl)-2-thiohydantoin **(4)** (ChiralPak IA as the stationary phase, 95:5 Hex:EtOH as the eluent, flow rate : 0.8 ml/min, column temperature: 7°C) (a) the recrystallized product which shows the presence of four isomers, (b) the micropreparatively resolved **RM**, (c-d) conversion of **RM** to **SM** with time in **ethanol** at 313 K. (*) The assignments have been done with comparison by the ^{1}H-NMR spectrum.

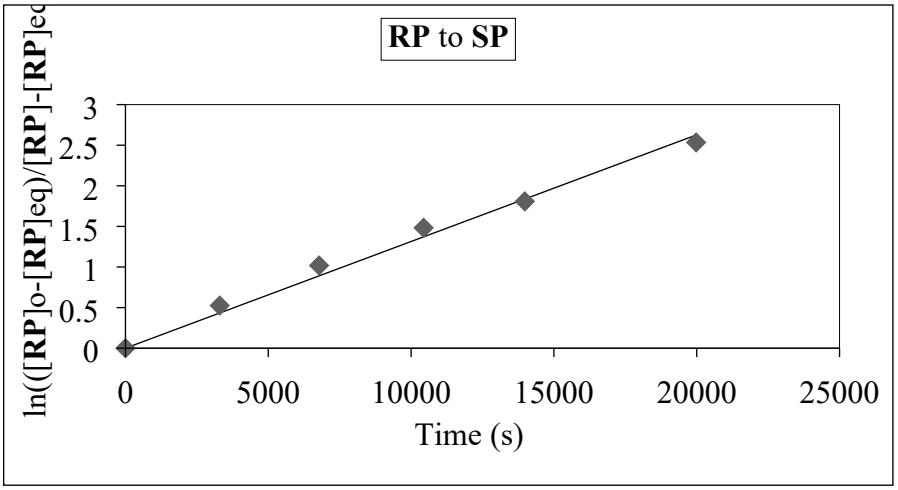

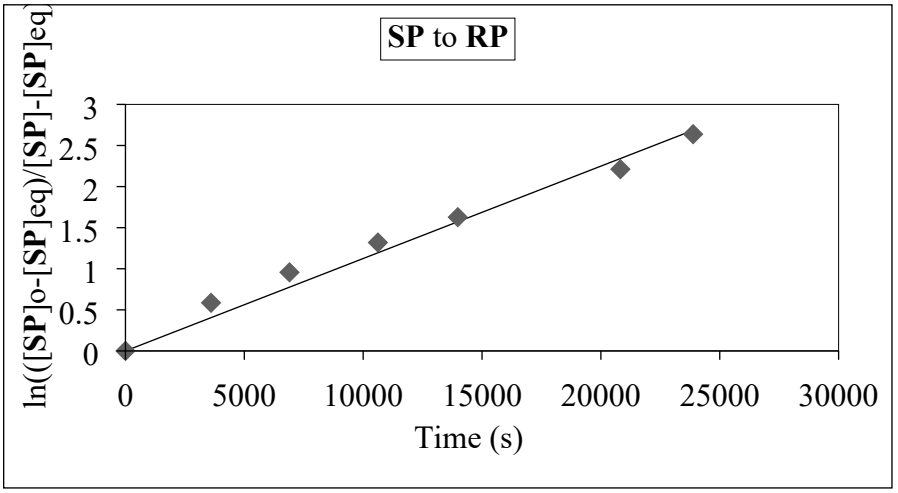

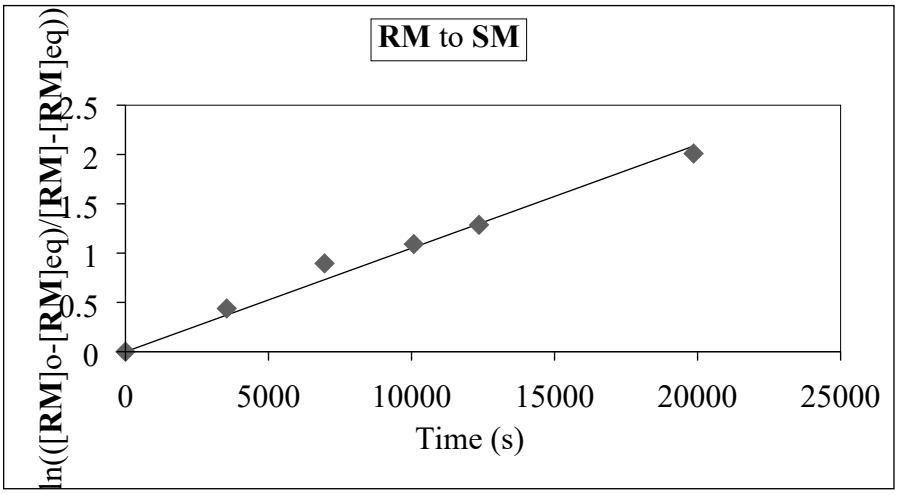

Fig. S18 The plot of ln(([**RP**]o-[**RP**]eq)/[**RP**]-[**RP**]eq)) , ln(([**SP**]o-[**SP**]eq)/[**SP**]-[**SP**]eq)), ln(([**RM**]o-[**RM**]eq)/[**RM**]-[**RM**]eq)) , versus time in **ethanol** at 313 K for 5-isobutyl-3-(*o*-bromophenyl)-2-thiohydantoin **(4)**.

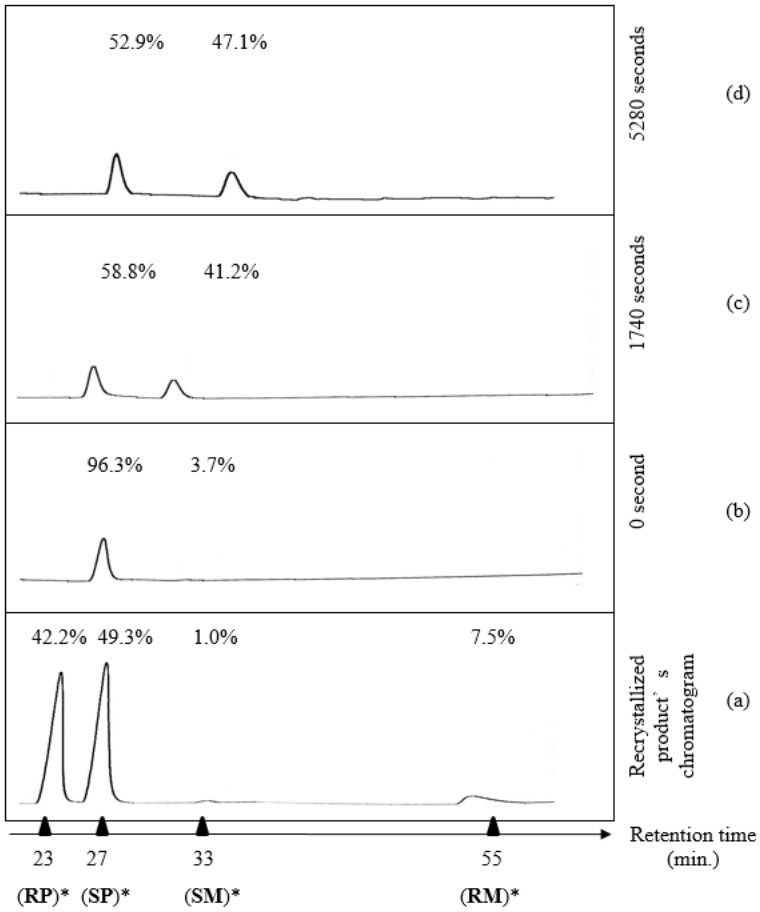

Fig. S19 HPLC chromatograms of 5-isobutyl-3-(*o*-bromophenyl)-2-thiohydantoin **(4)** (ChiralPak IA as the stationary phase, 95:5 Hex:EtOH as the eluent, flow rate : 0.8 ml/min, column temperature: 7°C) (a) the recrystallized product which shows the presence of four isomers, (b) the micropreparatively resolved **SP**, (c-d) conversion of **SP** to **SM** with time in **toluene** at 383 K. (*) The assignments have been done with comparison by the ^{1}H-NMR spectrum.

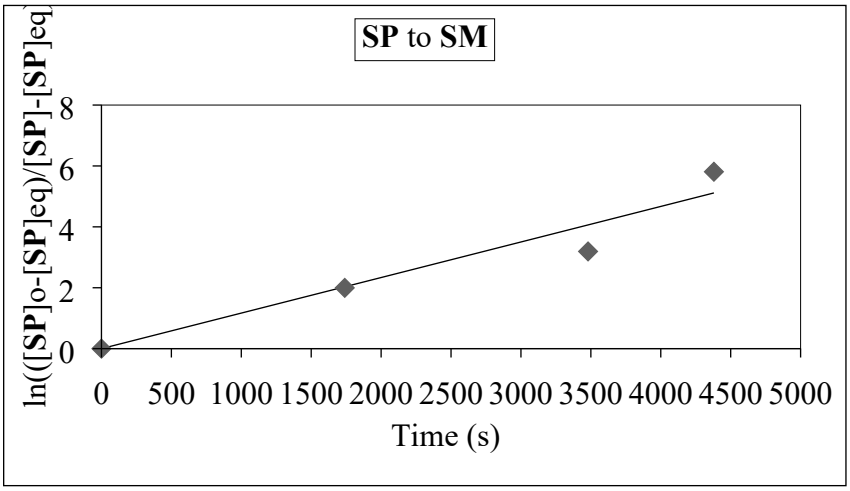

Fig. S20 The plot of ln (([**SP**]o-[**SP**]eq)/[**SP**]-[**SP**]eq)) versus time in **toluene** at 383 K for 5-isobutyl-3-(*o*-bromophenyl)-2-thiohydantoin **(4)** .

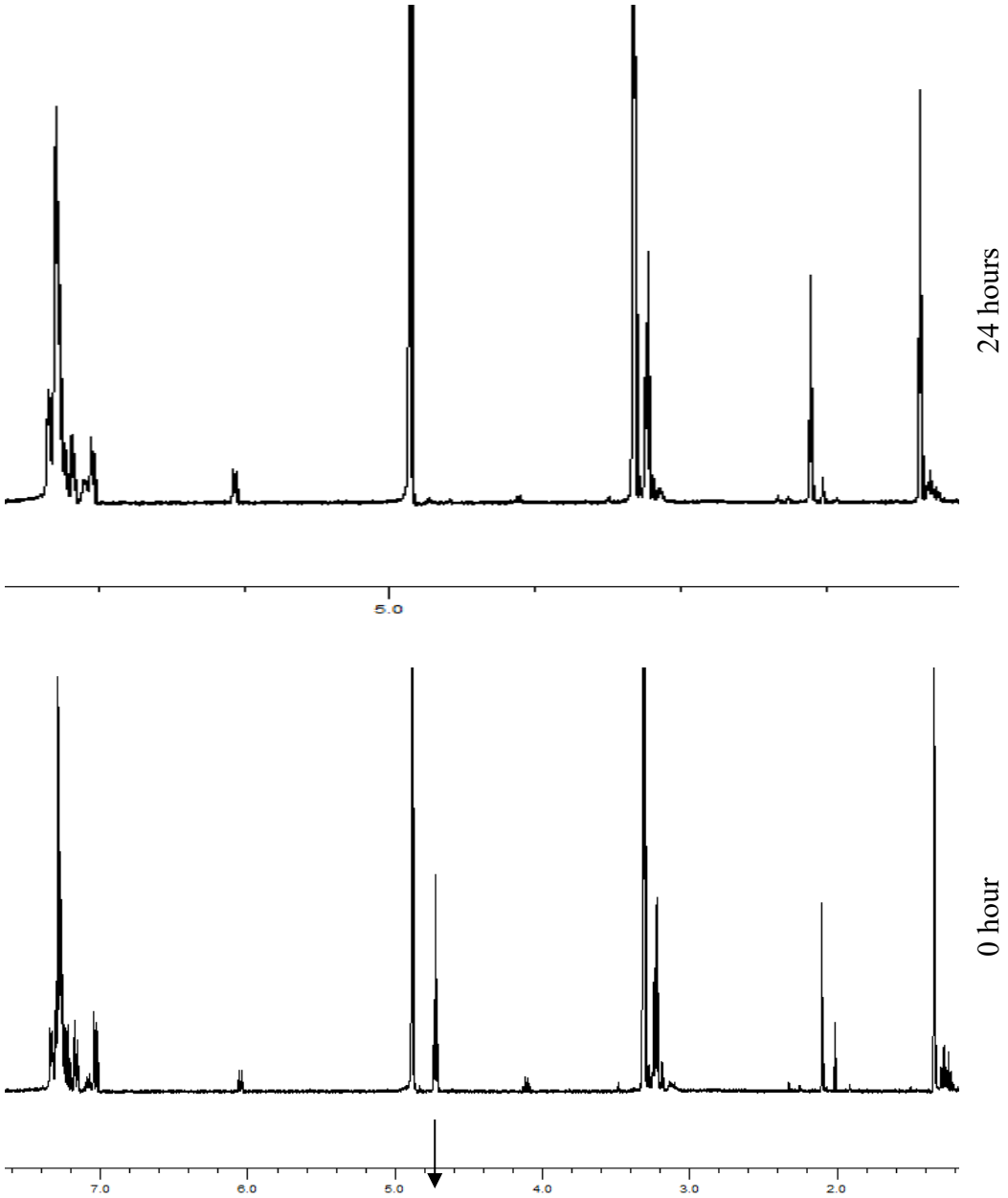

C-5 signal

Fig. S21 5-benzyl-3-(*o*-tolyl)-2-thiohydantoin (**1**) C-5 hydrogen signal change with time in CD_3OD.

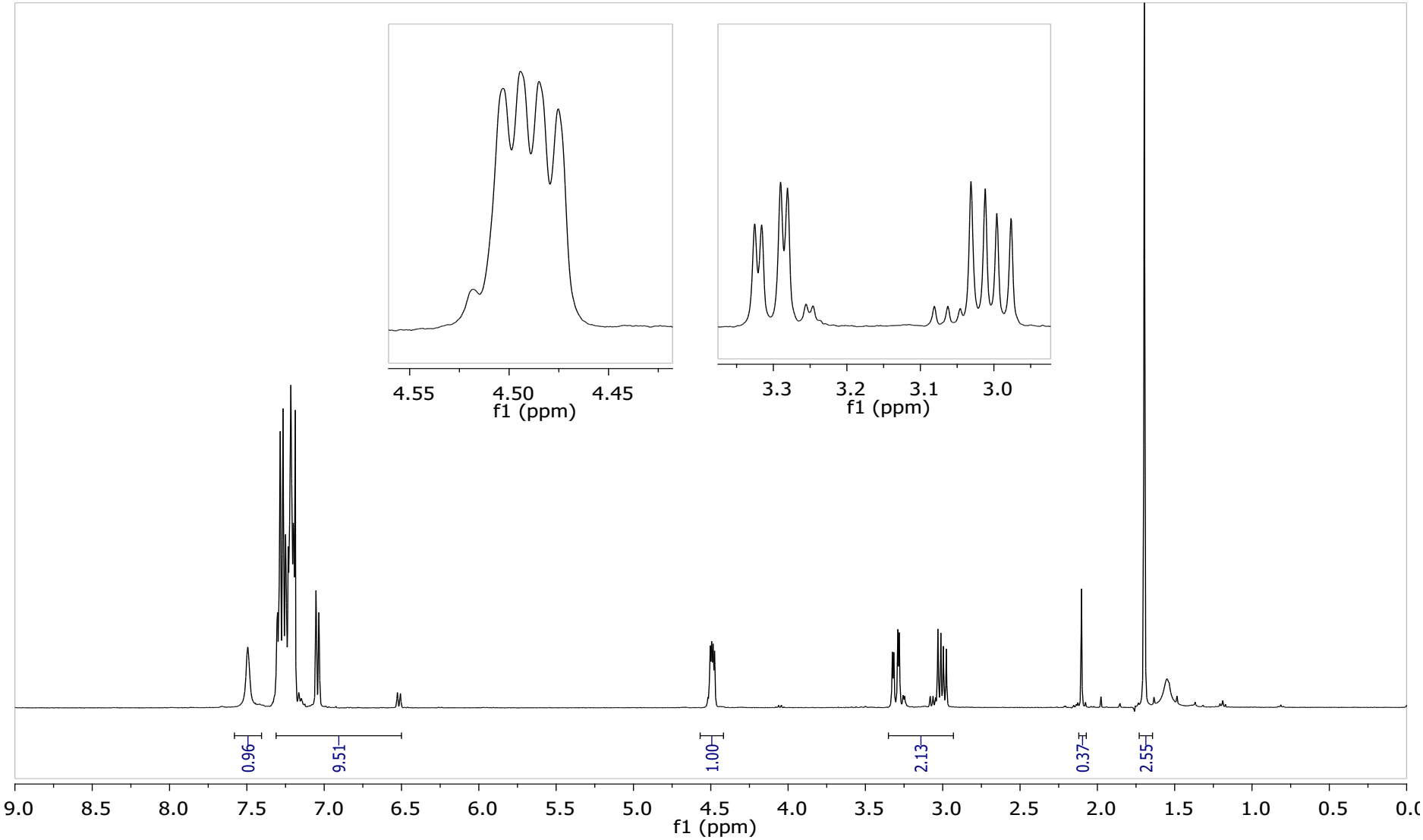

Fig. S22 ^{1}H NMR spectrum of 5-benzyl-3-(*o*-tolyl)-2-thiohydantoin **(1)** in $CDCl_3$

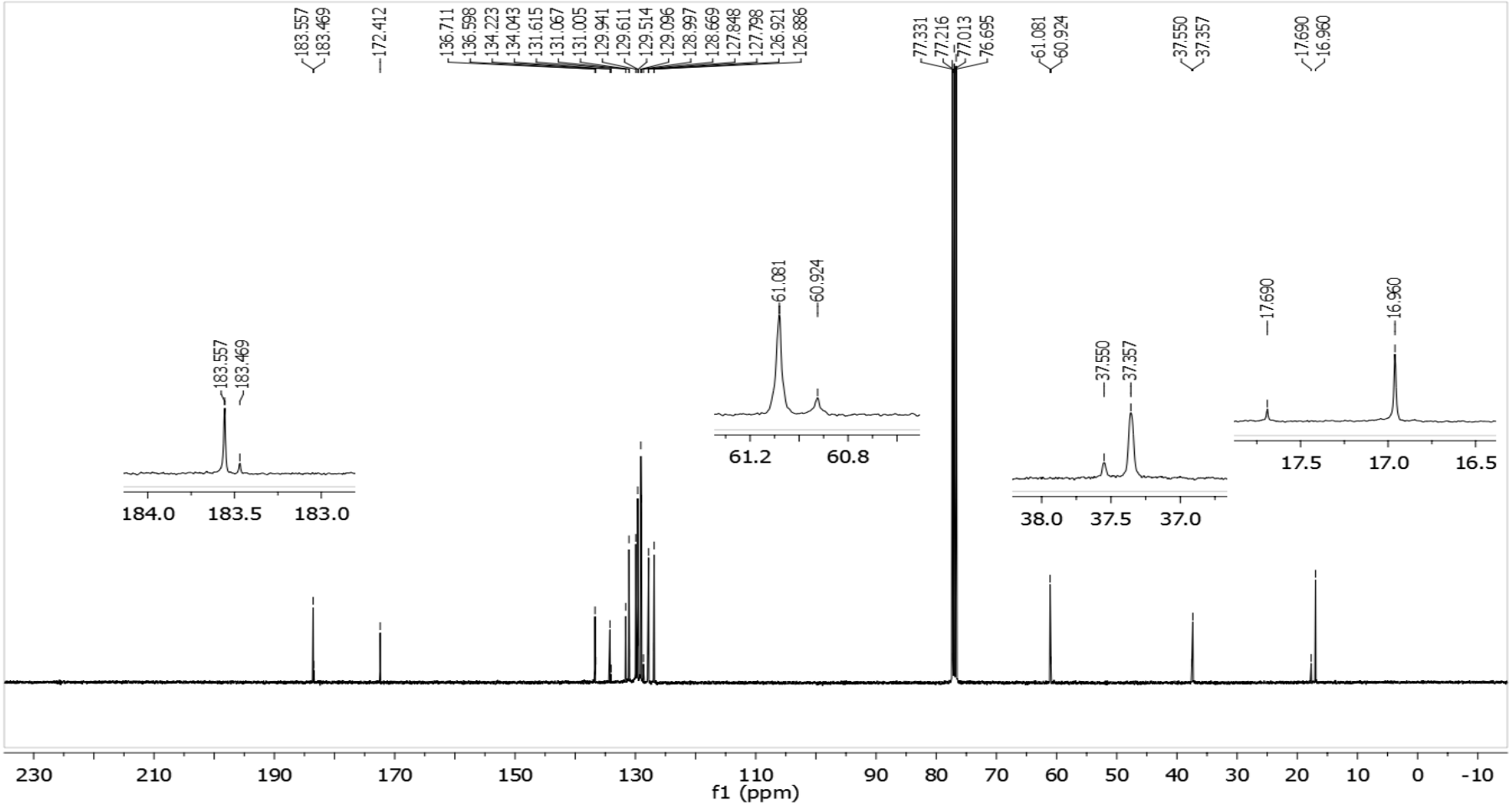

Fig. S23 ^{13}C NMR spectrum of 5-benzyl-3-(*o*-tolyl)-2-thiohydantoin **(1)** in $CDCl_3$

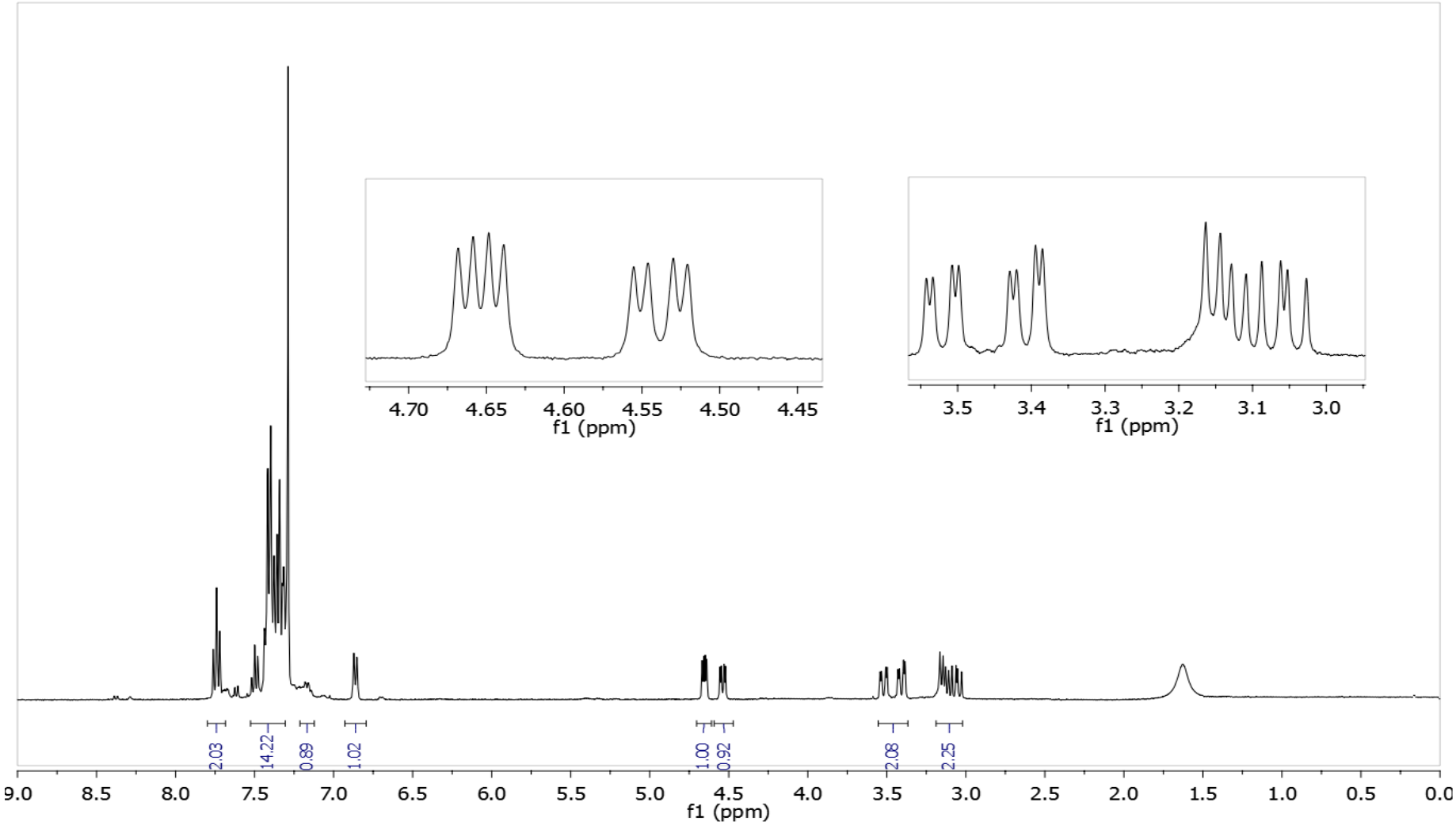

Fig. S24 ^{1}H NMR spectrum of 5-benzyl-3-(o-bromophenyl)-2-thiohydantoin **(2)** in $CDCl_3$

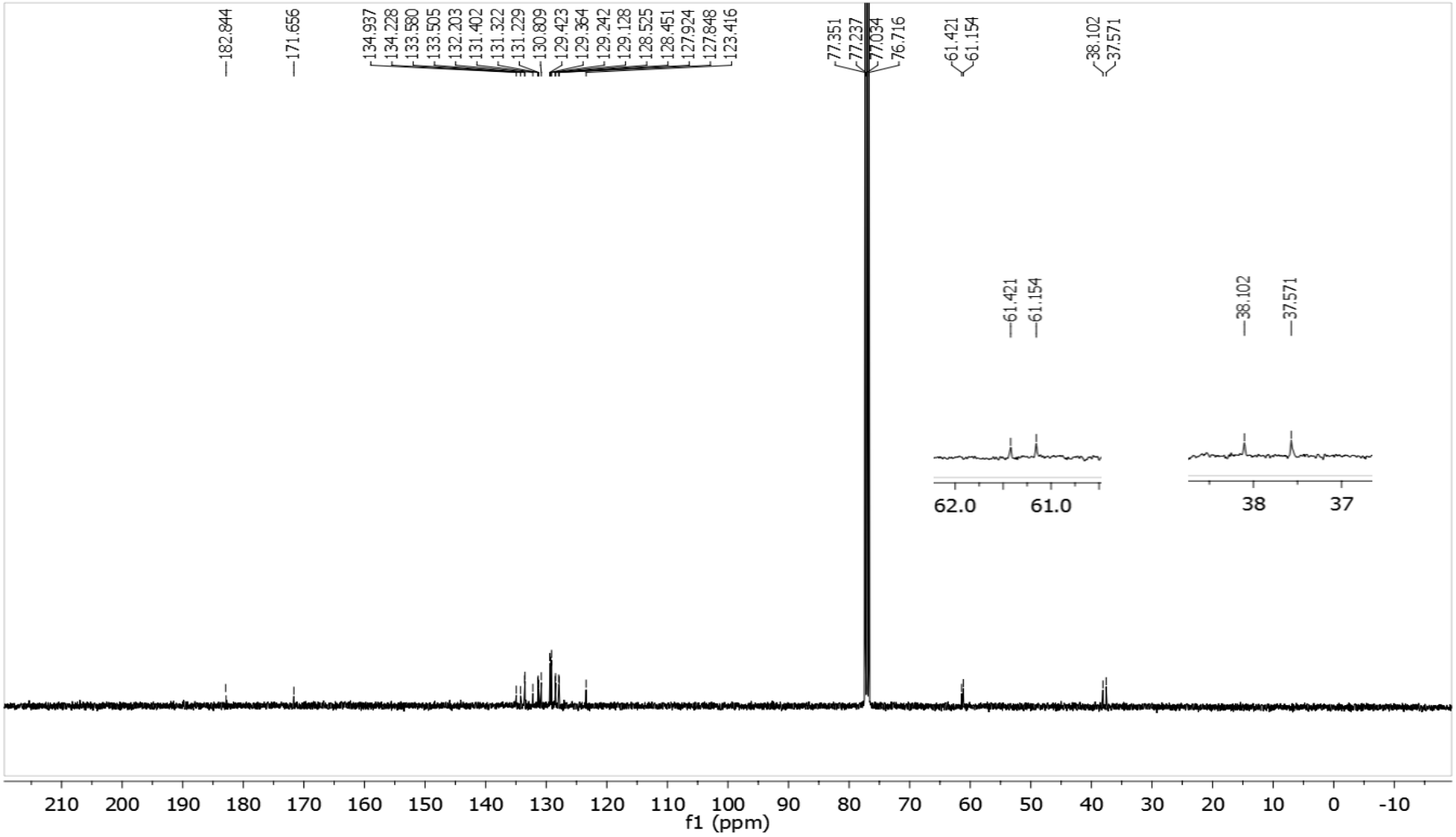

Fig. S25 ^{13}C NMR spectrum of 5-benzyl-3-(o-bromophenyl)-2-thiohydantoin **(2)** in $CDCl_3$

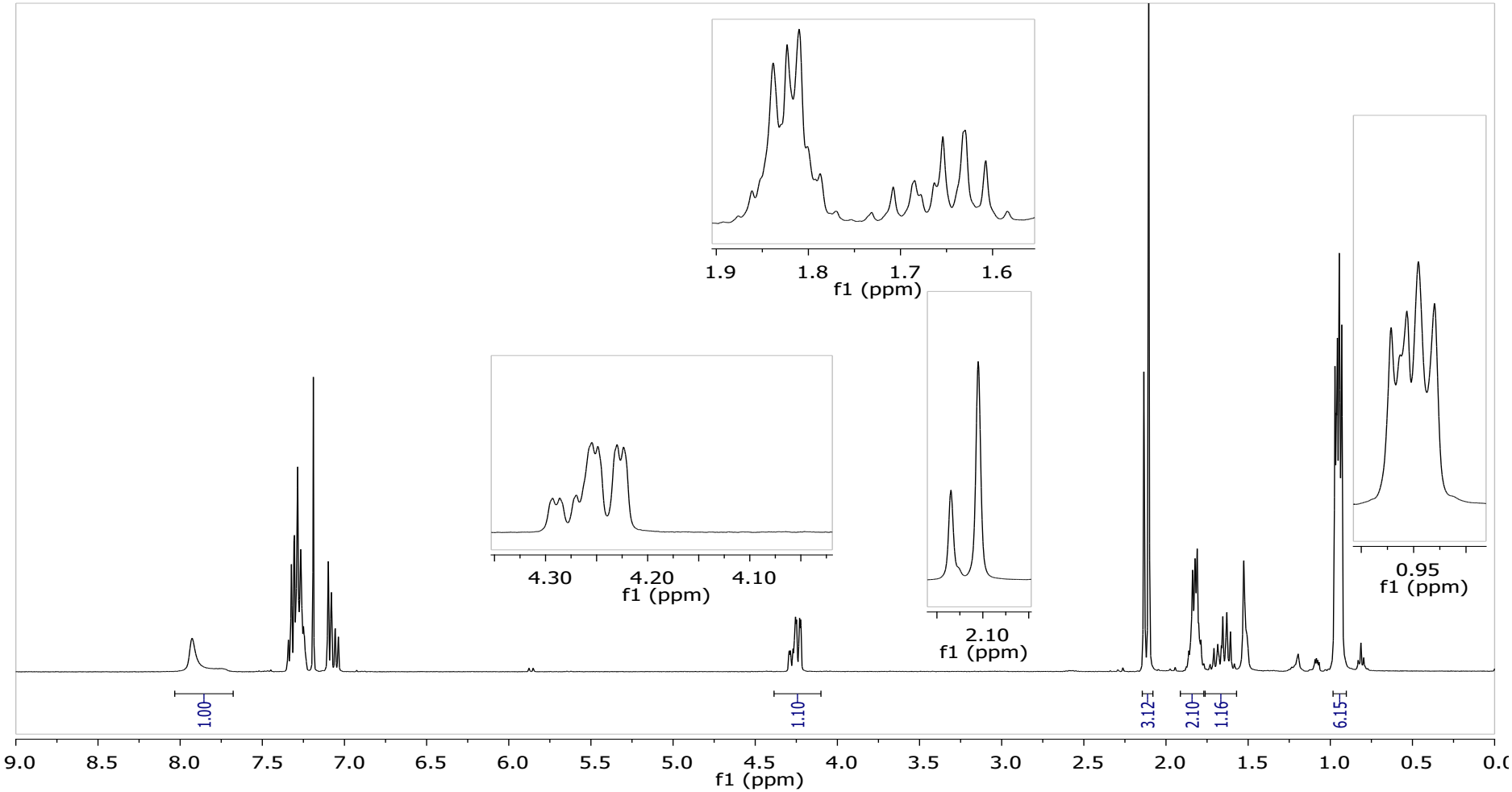

Fig. S26 ^{1}H NMR spectrum of 5-isobutyl-3-(*o*-tolyl)-2-thiohydantoin **(3)** in $CDCl_3$.

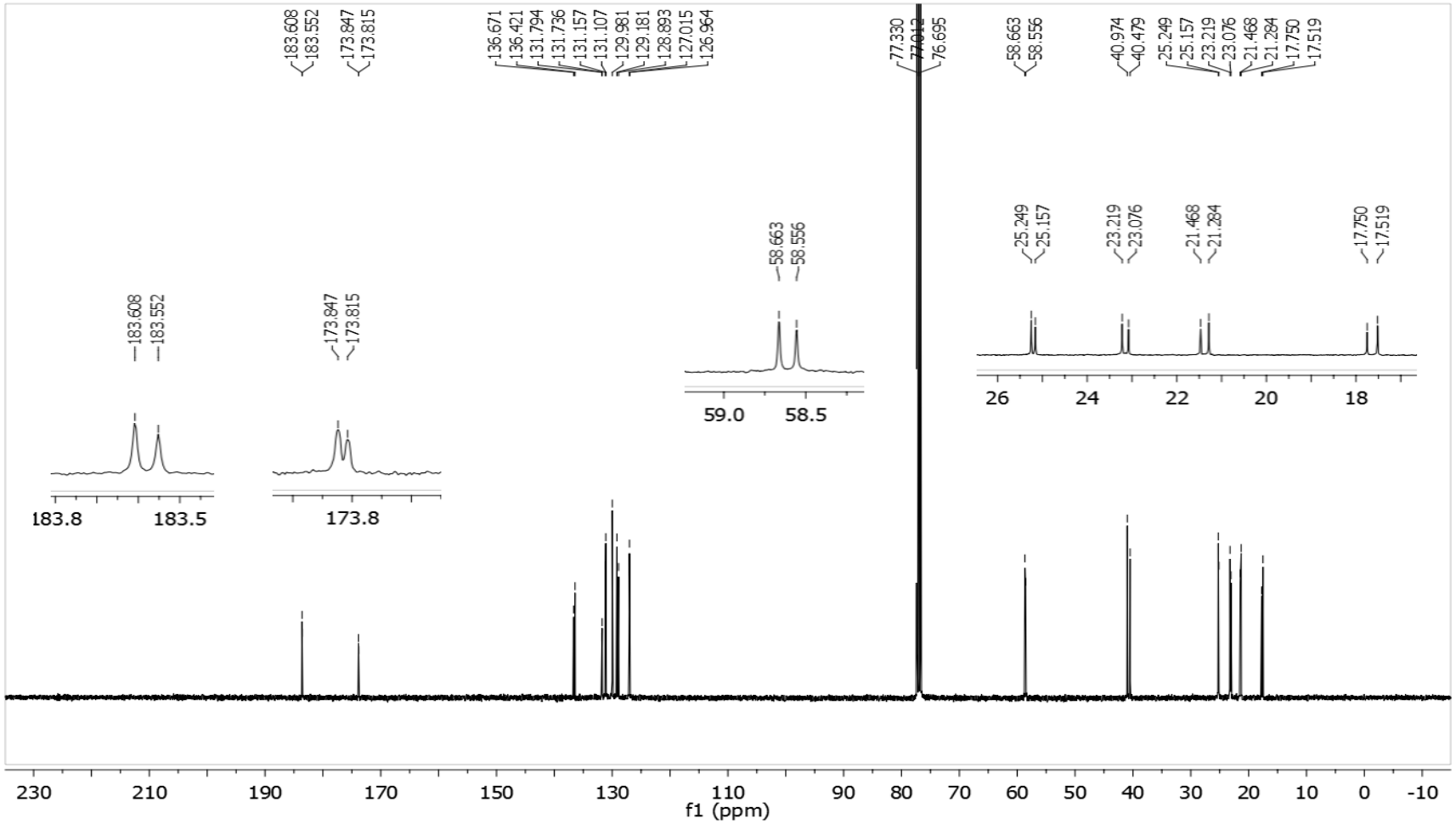

Fig. S27 ^{13}C NMR spectrum of 5-isobutyl-3-(*o*-tolyl)-2-thiohydantoin **(3)** in $CDCl_3$.

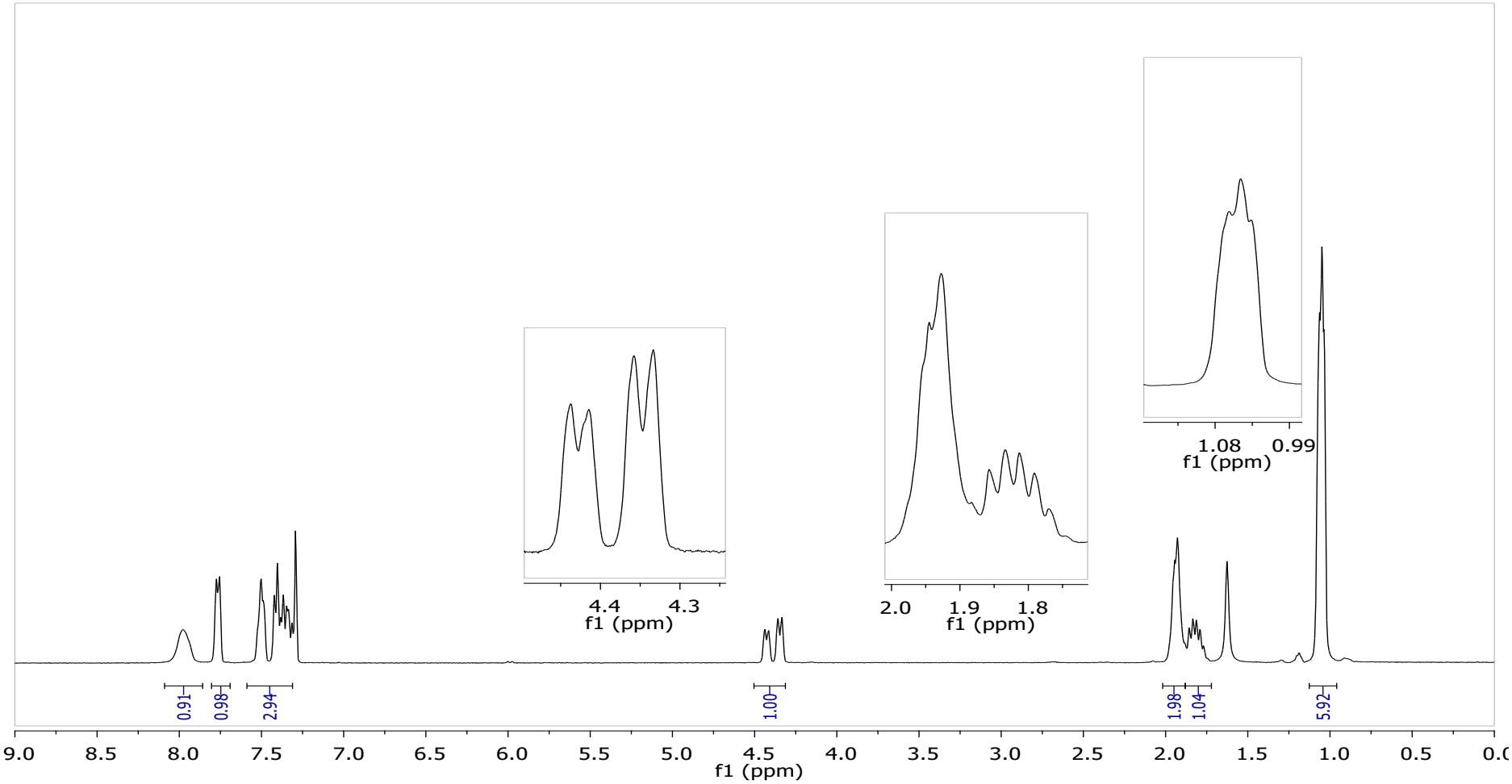

Fig. S28 ^{1}H NMR spectrum of 5-isobutyl-3-(o-bromophenyl)-2-thiohydantoin **(4)** in $CDCl_3$.

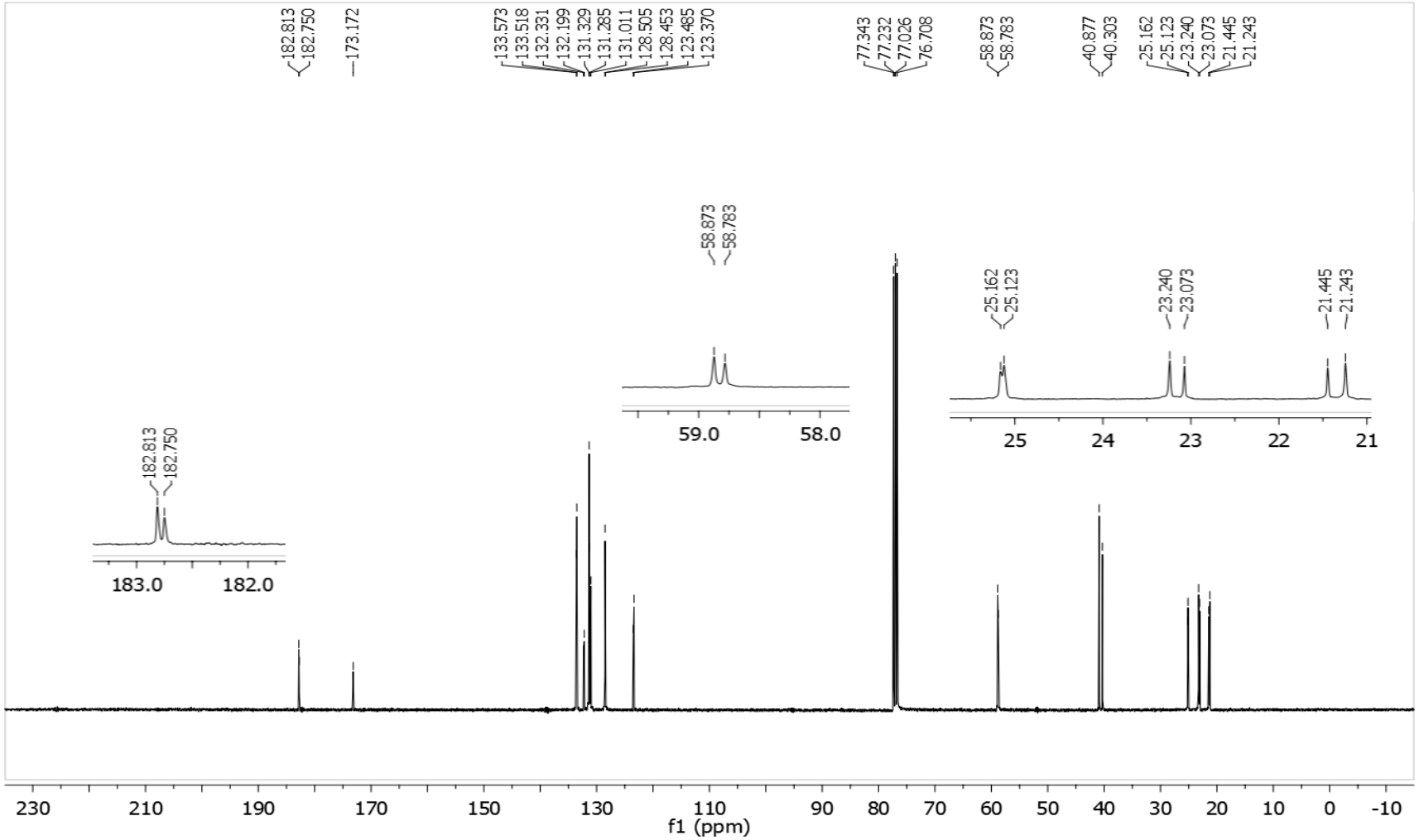

Fig. S29 ^{13}C NMR spectrum of 5-isobutyl-3-(o-bromophenyl)-2-thiohydantoin **(4)** in $CDCl_3$.

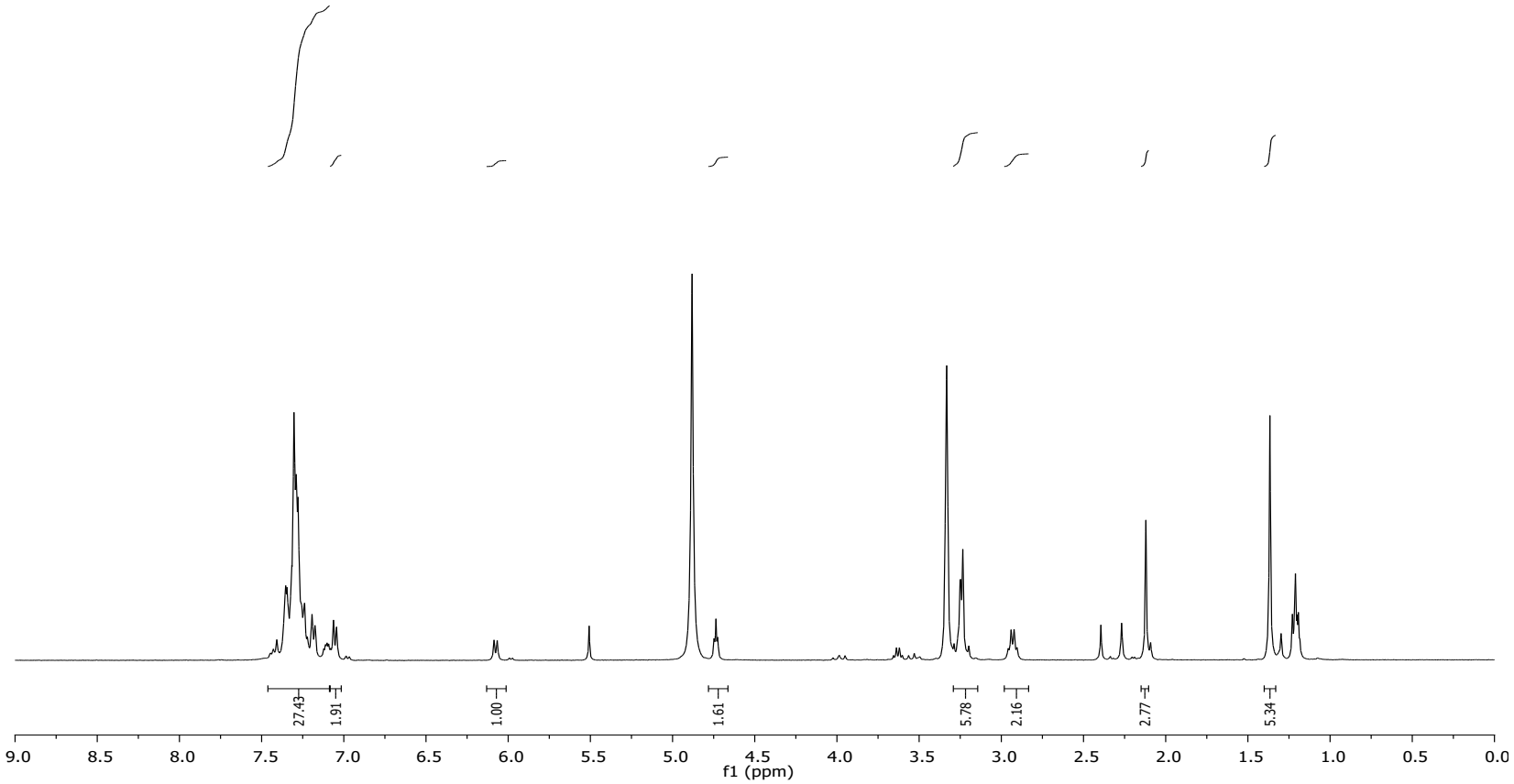

Fig. S30 ^{1}H NMR spectrum of 5-benzyl-3-(*o*-tolyl)-2-thiohydantoin **(1)** (crude) in methanol-d_4.

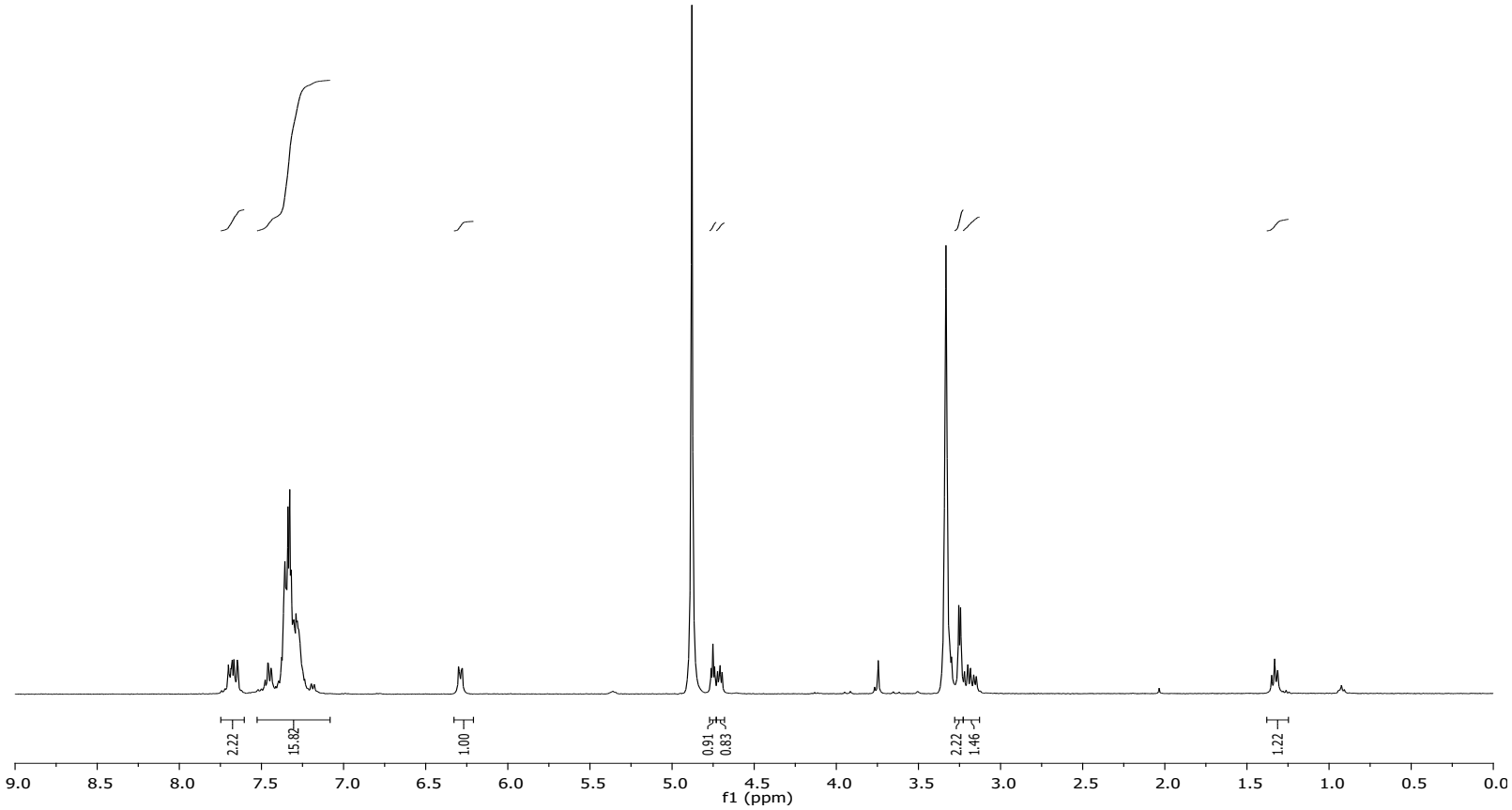

Fig. S31 ^{1}H NMR spectrum of 5-benzyl-3-(o-bromophenyl)-2-thiohydantoin **(2)** (crude) in methanol-d_4.

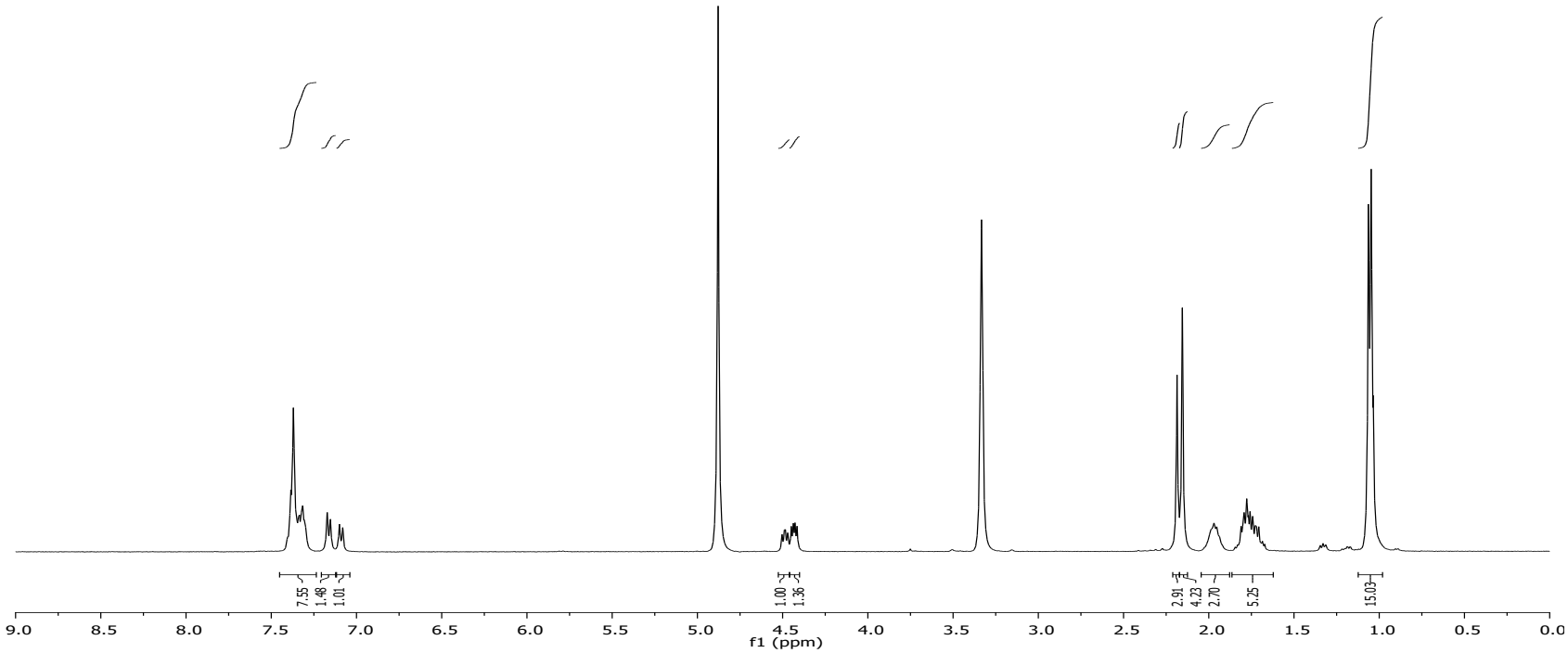

Fig. S32 ^{1}H NMR spectrum of 5-isobutyl-3-(*o*-tolyl)-2-thiohydantoin **(3)** (crude) in methanol-d_4.

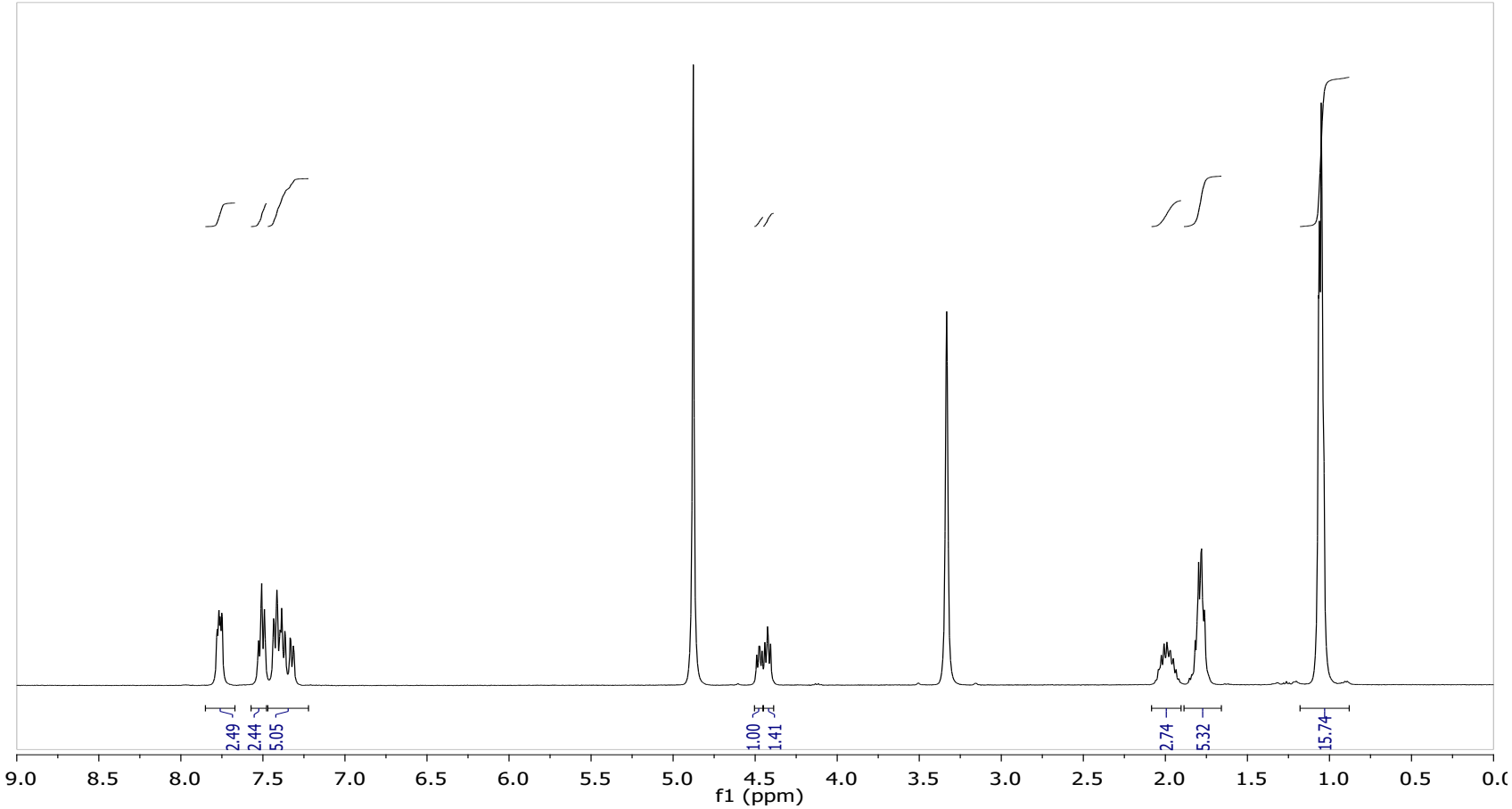

Fig. S33 ^{1}H NMR spectrum of 5-isobutyl-3-(o-bromophenyl)-2-thiohydantoin **(4)** (crude) in methanol-d_4.